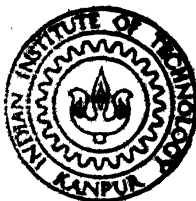


# A PHOTOVOLTAIC INDUCTION MOTOR WATER PUMP AND FAN DRIVE

by  
NASEAM HAIDER JAFRI

EE  
1987  
M  
JAF  
PHO

Th  
EE/1987/14  
N 18 P



DEPARTMENT OF ELECTRICAL ENGINEERING

INDIAN INSTITUTE OF TECHNOLOGY, KANPUR

MAY, 1987

# **A PHOTOVOLTAIC INDUCTION MOTOR WATER PUMP AND FAN DRIVE**

**A Thesis Submitted  
In Partial Fulfilment of the Requirements  
for the Degree of  
MASTER OF TECHNOLOGY**

**by  
NASEAM HAIDER JAFRI**

**to the  
DEPARTMENT OF ELECTRICAL ENGINEERING  
INDIAN INSTITUTE OF TECHNOLOGY, KANPUR  
MAY, 1987**

Lovingly  
dedicated  
to  
My parents and teachers'

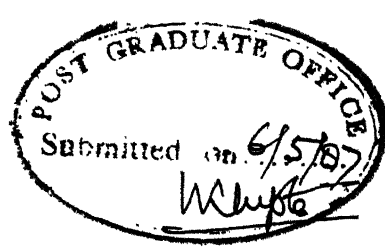
CENTRAL LIBRARY

Acc. No. 2..... 98326

The &ic  
621.3124  
J'8p

EE- 1907- M- JAF- PHO

14



## CERTIFICATE

This is to certify that the thesis entitled  
'A PHOTOVOLTAIC INDUCTION MOTOR WATER PUMP AND FAN DRIVE'  
is a record of work carried out under our supervision  
by Naseem Haider Jafri and that it has not been submitted  
elsewhere for a degree.

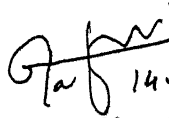
— — —  
( Dr. G.K. Dubey )  
Professor

— — —  
( Dr. G.C. Ray )  
Assistant Professor

Department of Electrical Engineering  
Indian Institute of Technology  
KANPUR

### ACKNOWLEDGEMENT

I express my deep sense of gratitude to Dr. GK Dubey and Dr. GC Ray for having suggested this very interesting topic, for their invaluable guidance, for providing an excellent working atmosphere and for their availability for discussion, whenever I needed throughout this work. I thank Mr. B.H. Khan, Ashwin, Reddy, Verma, Dutta, Dhoria, Rais, Mukesh, KK Islam and scores of other friends whose constant encouragement and help were useful. My thanks are due to Mr. J.A. Usmani, ML Gupta, Munna, OP Arora, DN Joshi and staff of the ACES Workshop, Central Workshop and electrical stores for their help at various stages of this work. In last but not least my thanks are due to Mr. JS Rawat for his neat and timely typing.

  
14.05.87  
Naseem H. Jafri

## ABSTRACT

Generally permanent magnet dc motors are used in photovoltaic pump drive. The brushes and commutator require frequent replacement and maintenance. In the present work an induction motor pump drive is proposed, which over comes the above mentioned problems. A maximum power tracker is developed which ensures maximum power input to motor by controlling the modulation index of the inverter. The single phase permanent capacitor motor is used and is operated at ~~high~~ good efficiency by using suitable speed control scheme. A single phase inverter is designed with least possible number of power transistors. A P.M technique operating at high frequency is employed to obtain sinusoidal output voltage and current with low harmonic distortion. A prototype drive is built in the laboratory and is tested with fan loads. The performance of the drive is found satisfactory.

## CONTENTS

	Page
<b>Chapter 1 INTRODUCTION</b>	<b>1</b>
1.1 Introduction	1
1.2 Organisation of thesis	3
<b>Chapter 2 PHOTOVOLTAIC PUMP?AND FAN DRIVE</b>	<b>4</b>
2.1 Introduction	4
2.2 Solar Cells	5
2.3 <del>2e2.1</del> General	5
2.2.2 Maximum power tracking	8
2.2.3 Conversion efficiency	11
2.3 Motors	13
3.2.1 D.C. motor	13
2.3.2 Induction motor	15
2.3.3 Synchronous motor	16
2.4 Pumps	17
<b>Chapter 3 PROPOSED DRIVE SCHEME</b>	<b>18</b>
3.1 Introduction	18
3.2 PV array module	20
3.3 Inverter	22
3.4 Control scheme	29
3.4.1 Control of modulation index	30
3.4.2 Control of frequency	32

	Page
Chapter 4 CONTROL AND PROTECTION CIRCUITS	37
4.1 Firing circuit	37
4.2 Base driver circuit	43
4.3 Voltage control oscillator	45
4.4 Maximum power tracker circuit	47
4.5 Protection circuit	53
4.5.1 Turn on snubber circuit	54
4.5.2 Turn off snubber circuit	56
4.6 Experimental set up	57
Chapter 5 PERFORMANCE OF DRIVE	60
5.1 Analysis of single phase permanent capacitor motor	60
5.2 Performance of inverter	64
5.3 Performance of drive	67
Chapter 6 CONCLUSIONS	71
APPENDIX I	73
REFERENCES	76

## LIST OF FIGURES

Fig. No.	Caption	Page
2.2.1a	Characteristics of solar cell with changing insolation	9
2.2.1b	Characteristics of solar cell with changing temperature	9
3.1.1	Proposed drive scheme	21
3.2.1	Oscillogram showing characteristics of PV array	23
3.3.1a	High frequency link resonant inverter	21
3.3.1b	High frequency link inverter	26
3.3.2	Single stage inverter	26
3.3.3	Inverter circuit	27
3.4.1	PV array characteristics and load line	34
3.4.2a	Speed-torque characteristics of permanent capacitor induction motor with variable voltage	34
3.4.2b	Speed-torque characteristics of permanent capacitor induction motor with constant V/F ratio	36
4.1	PV induction motor pump drive	38
4.1.1	PWM pattern generation	38
4.1.2	Firing circuit	41
4.1.3	Waveforms at different points of firing circuit	42
4.2.1	Optical isolator	44
4.2.2	Isolated power supply	44
4.2.3	Base drive circuit	46
4.3.1	VCO circuit	46

Fig. No.	Caption	Page
4.4.1	Maximum power tracker circuit	49
4.4.2	Waveforms of maximum power tracker circuit	52
4.5.1	Inverter circuit with snubbers	55
4.6.1	Detailed control circuit	58
4.6.2	Experimental setup	60
5.1.1	Characteristics of 1 phase permanent capacitor induction motor, Motor I	65
5.1.2	Characteristics of 1 phase permanent capacitor induction motor, Motor II	65
5.2.1	Oscillograms of inverter performance	66
Table I	Experimental results	69

## CHAPTER 1

### INTRODUCTION

#### 1.1 *Introduction*

Water is pumped for drinking, irrigation and for the industry and use in households. The cost of the water is directly related to the required energy for pumping of the water from the ground. The common energy for water pumping is the electrical energy due to its availability near the site of human habitation at reasonable cost. However in small villages and agriculture fields, where conventional power grid supply is not available, diesel pump sets are used for water pumping. These pump sets require frequent maintenance and fuel. The annual running cost becomes principal economy factor. There is vast need for low cost systems, which requires no fossil fuel and very little maintenance specially in India due to its poor reserves of fossil fuels. Such system must employ reliable equipment to ensure high MTBF (mean time between failure). The photovoltaic system has the potential to provide such an alternative. However, initial capital cost of the photovoltaic pump system is about four times the diesel alternative, but the difference can be recovered in four years (assuming no increase in the cost of diesel) [8]. Furth

reduction in the cost of the solar cells is expected due to the large scale production and advances in manufacturing techniques. Therefore the future of such systems is very bright.

Photovoltaic pump system consists mainly three components, electric source which is a solar cell array, an electromechanical converter which is an electric motor and load which is a centrifugal pump. Several pump systems have been developed, which employ dc permanent magnet [7] or wound field motors [9-11]. These drives require frequent maintenance due to replacement of the brushes and commutator. Some authors have suggested ac permanent magnet motor but the reliability of such system at this stage may be considerably poor due to involvement of complex electronics; ~~which eliminates both~~

In the present work, photovoltaic induction motor pump drive which eliminates both of the above mentioned problems has been investigated. It is a variable speed drive with a maximum power tracker in the inverter circuit, to ensure the maximum use of available photovoltaic power. A single phase transistor inverter with least possible power switches is fabricated and tested on the single phase permanent capacitor induction motor coupled with fan.

## 1.2 ORGANISATION OF THE THESIS

In chapter 2 the operation and behaviour of solar cell and different motors is briefly discussed. The advantage and disadvantage of various drive schemes and maximum power tracking schemes is also outlined.

In Chapter 3 the proposed drive scheme is described. The operation and design of the single phase transistor inverter is discussed. The principal of the power maximization is also discussed.

Chapter 4 deals with the details of control and protection circuits. The design and operation of the firing, base drive, maximum power tracker and snubber circuits is described.

In Chapter 5 analysis of the single phase permanent capacitor induction motor with voltage source is discussed. The experimental results of the drive are presented. Also some oscillogram<sup>s</sup> of the inverter performance with different loads is presented.

## CHAPTER 2

### PHOTO VOLTAIC PUMP AND FAN DRIVE

#### 2.1 INTRODUCTION

The conventional sources of energy are used either directly converted into electricity to supply the demand of energy in present age. The direct use of energy involves burning fuels such as wood, gas, oil and coal directly for the purpose of heating requirement or in combustion engine for the purpose of doing mechanical work. Mostly electricity is created by converting energy from fossil fuels and nuclear reactions into electrical energy through the production of steam and the rotation of a generator. The conversion procedure is costly and inefficient. Both the cases suffer from the disadvantage of health hazard due to radioactive radiation and/or pollution. Since the demand of energy is increasing at an alarmingly high rate and the conventional sources of energy are very limited, there is a need of non-conventional sources of energy which should be economical, unlimited and free of all types of pollution. The solar energy is a one and easy conversion into electricity without any of the promising alternative due to its availability all any

suffers from the limitations such as cost of solar cell, the amount of annual sunshine at the site, the time and type of photo-voltaic output and the space required to generate significant amount of power.

Up till now solar cells have been used for satellites, electric calculators and watches, single person airplane, prototype cars, water pumping, water desatination plant and professional radio stations [1]. Small water pumping irrigation projects are most suitable for remote locations in India. A simple photovoltaic water pump drive consists of solar cell module, a motor and a pump. In this chapter these components of drive will be discussed.

## 2.2 SOLAR CELLS

### 2.2.1 General:

The solar cell was reported as early as 1941 but it was 1954 when silicon solar cell was announced by Chapen, Fuller and Pearson. The solar cell was widely used in space applications by 1960. By the end 1970's, the production of silicon cells for use in terrestrial applications became dominant factor and hence fast reduction in the cost due to large scale production. The basic principle of operation of solar cells

depend upon 'Photovoltaic effect' reported by Becquerel in 1839 [2-3]. The solar cell converts the sun light directly into electricity and heat plays no constructive part in the process. It is somewhat puzzling because all conventional methods of generation of electricity involve production of heat.

The best silicon solar cells are made from one carefully grown crystal in which all the atoms are facing the same direction and fit together into a neat three dimensional grid. Multicrystal or poly crystalline cells are less expensive to grow but have a lower efficiency. Amorphous silicon cells promises to be most inexpensive to manufacture because they can easily be produced in this film but their conversion efficiency is lower than that of single and polycrystalline cells. Beside silicon solar cells, there are some other solar cells having their own advantages and disadvantages. The copper-cadmium sulfide which are inexpensive in production but have low conversion efficiency of 9% and gallium arsenide with an efficiency of 22% are most common [1]. The basic principle of operation of solar cell is outlined below.

In a normal PN junction a small voltage called potential barrier is developed across the junction due to migration of

free electrons from N to P material and reverse flow holes.

↓  
This voltage prevents the further flow of charge carriers and sweeps away all the free electrons and holes from the depletion region. The number of majority carriers in both sides of junction will depend upon the level of doping but the number of minority carriers (holes in N type and electrons in P-type) will depend upon the light and heat condition. At the room temperature, there are free electrons and holes in the junction; these charge carriers either recombine if they are away from the junction or swept away by the potential barrier towards their majority concentration. In an unilluminated junction majority and minority carrier currents are equal and balance each other out. This balance of current is disturbed when light falls upon the junction. The each incident photon having energy  $E_h$  more than band gap energy  $E_g$  of silicon is capable of generating one electron hole pair. These electrons and holes will be forced apart by electric field and pushed towards their respective N and P material provided thickness of junction is small enough and life time of charge carrier is large enough to avoid recombination. This movement of electron-hole pair will give rise

to photo-voltaic current. Amount of current and hence power depends mainly upon the intensity of light, temperature and cell area. The short circuit current of solar cell is proportional to the intensity of light and cell area but varies little with temperature, while the open circuit voltage of solar cell is inversely proportional to the temperature and is not effected by the cell area. The open circuit voltage varies little with the intensity of light. The characteristic of solar cell and its variation with intensity of light and temperature is shown in Fig. 2.2.1.

### 2.2.2 Maximum Power Tracking:

A solar cell array is consists of many solar cells connected in a series/parallel fashion. The array has I-V characteristic similar to that of a single solar cell. Each I-V curve has a maximum power point at which the product of array voltage and current is maximum. It is advantageous always to operate the array at its maximum power point. Maximum power can be tracked by placing an electronic circuit called 'maximum power tracker' between solar cell array and the load; which changes the apperent impedance of load untill the photovoltaic power is maximized. The photovoltaic power

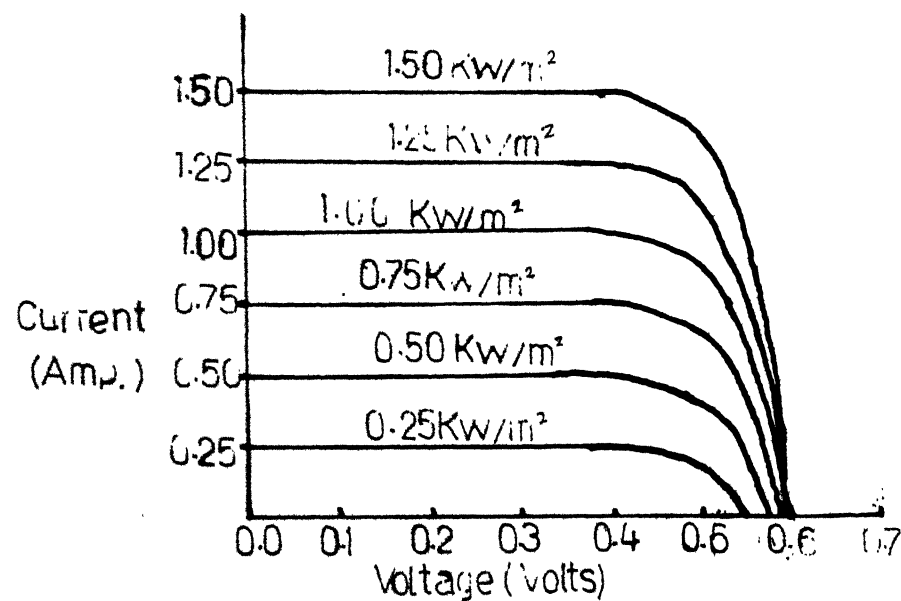


Fig. 2.2.1a Characteristics of solar cell with changing insolation

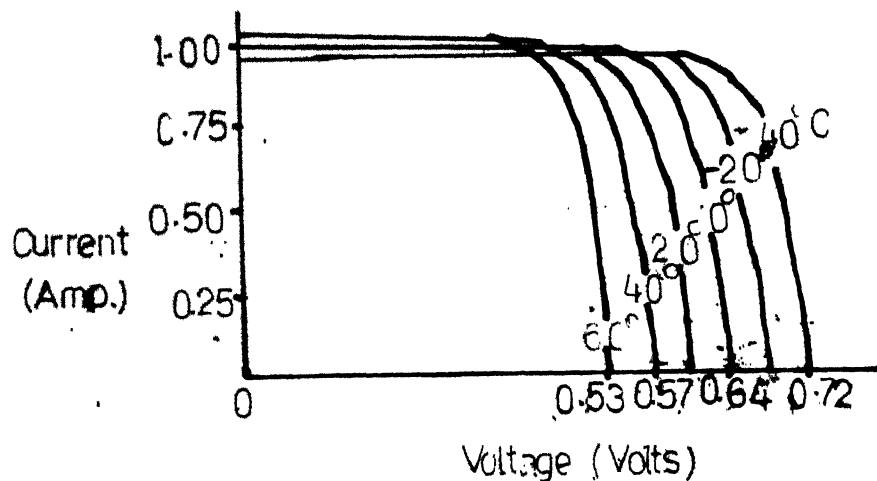


Fig. 2.2.1 b. Characteristics of solar cell with changing temperature

can be sampled either by multiplying the voltage and current readings of PV array together or in a special way by measuring just voltage or current. Several maximum power tracker are reported in literature employing single chip microcomputer [5-6].

The surface orientation of the PV array affects the amount of energy received from the sun and hence PV output power. The amount of direct beam solar energy that a surface receive can be optimized by keeping the surface at right angle to sun's direct radiation at all times. The cost of the energy and the mechanical assembly required to track the sun accurately and consistently each day generally outwieghs the extra energy obtained by doing so, when flate plate solar cell modules without concentratration are used [1]. The next alternative is to fix the surface of module so that the sun's angle on the plane is closest to the perpendicular most of the time. In the Northern Hemesphere an area facing due south at a tilt angle that equals to side's latitude would obtain the optimum amount of <sup>energy over</sup> the entire year. The solar energy can be maximized during winter months by increasing the tilt angle by  $11^\circ$  and in summer months by decreasing the tilt angle by  $11^\circ$ . However tilting a surface up from the

horizontal decreases the diffuse radiation and reflection received from the ground. Therefore for a precise optimum tilt angle the relative amount of the direct diffuse and reflected light must be known. The surface tilt angle need not be too precise because a <sup>e i a</sup> deviation of as much as  $10^{\circ}$  from optimum tilt angle will produce a decrease in incident solar energy little more than 5% of maximum [1].

### 2.2.3 Conversion Efficiency:

Amount of the PV power output of solar cell array depend upon the amount of the solar energy and conversion efficiency of the solar cell. The solar power received directly outside the atmosphere is continuous at a rate of about 1350 watts/ $m^2$  and is known as solar constant. The solar power level received on the earth fluctuates due to rotation of earth at its axis and around the sun. The peak solar power experienced on a horizontal surface near sea level is about 1000 watts/ $m^2$  and is called one sun at which solar cells usually are rated. The conversion efficiency of a solar cell is only about 15%. The theoretical maximum efficiency is about 25%. Major factors responsible for low conversion efficiency are as follows [1-4].

- a) The sun light consists of photons having different energies. The photon having energy less than the band gap energy of silicon passes straight through crystal with no effect. This wastes about 24% of solar energy.
- b) Since each incident photon having energy more than band gap energy of silicon is capable of generating one and only one electron hole pair, hence over energetic photon does nothing but make the crystal hot. This waste another 32% of solar energy.
- c) Despite of antireflection coating about 3% of incident energy is lost through reflection. Recombination of electron hole pair due to impurities in crystal and limited life time, and absorption of photons away from the depletion layer causing heat, accounts for another 20% unavoidable losses.

The above mentioned first two factors are inherent with the silicon solar cell. The latter two factors can be limited by clever design but can not be eliminated.

A stand alone photovoltaic power system needs some form of energy storage and/or auxiliary power supply to supply the load demand during night or cloudy day. The general practical technology for electric storage is Lead acid batteries which are inefficient and expensive. The next alternative is public

utility grid whenever possible. For the application of water pumping instead of electric power, water can be stored in a tank or reservoir. This form of storage is most economical and efficient. Moreover solar cells generate power in direct current form which may be converted to ac form by a static inverter. A maximum power tracker may be incorporated in the circuit to ensure maximum possible PV power.

## 2.3 MOTORS

For a photovoltaic water pumping system, one can employ dc motor, induction motor or synchronous motor. All of them have their own advantages and disadvantages. In the following paragraph these will be discussed.

### 2.3.1 D.C. Motors:

The most commonly used motor for photovoltaic pumping systems are d.c. motors. The permanent magnet dc motors are preferred due to their high full load and part load efficiency. The permanent magnet dc motors have the full load and part load efficiencies in the range of 78-87% and 66 to 78% for a motor of rating 400W. The full load efficiency of a typical ac induction motor is in the range of 25-65% and that of field wound dc motor would be 65 to 70% for the same power rating.

Despite their high cost, dc drives employing permanent magnet dc motors are cheaper than ac drive or field wound dc drive due to their high efficiency which result in reduction of solar array area [7,8]. All type of dc motors suffer from the disadvantage of brushes and commutation. Generally such machine require new brushes at <sup>an</sup> interval of the order of 2000 - 4000 hours and if this is not done some motor can suffer irreparable damages. Certain dc motors are being offered with claimed brush lives of about 10,000 hours and is to be tested in field conditions. The two alternative schemes are possible for dc drive, either by direct connection of PV array to the dc motor or by connecting a dc to dc converter between PV array and the dc motor. Maximum power can be ensured from the PV array by manual adjustment of the series/parallel combination in the former case and by incorporating a maximum power tracker circuit in the latter case. However UNDP project report recommend the manual adjustment. Several approaches for direct connection of the PV array and dc motor has been reported in literature such as graphoanalytic method for series, shunt and separately excited field wound dc motor [9-10] and analytical analysis of series excited field wound motor [11]. The direct connection of dc motor and PV array requires less number of components hence it is efficient and economical but

suffers from the serious limitation of proper matching of the different components and dependence on the site parameters for good performance. On the other hand one has to sacrifice the efficiency when dc to dc converter with <sup>max</sup> man power tracker is employed. For the best choice a comparative study of both scheme is required.

### 2.3.2 Induction Motor:

The induction motor offer certain advantages over the dc motor such as low cost, low maintainance due to absence of brushes and commutator, rigid and robust construction but suffers from the disadvantage of low full load and part load efficiency in low power rating. However for the motor ratings greater than 1 KW, the efficiency is comparable with field wound dc motor. Since PV power is in direct current form, an expensive inverter is needed, when ac motors are employed. In low power rating single phase induction motors are used due to their general availability. Permanent capacitor motors are prefered due to their high power factor, which reduces the rms rating of power switches used in the inverter. In low power applications inverters are realized by employing power transistors or MOSFET's using PWM technique at high frequencies. The basic drive scheme may

consists of a PV array, PWM inverter and induction motor. However maximum power from the PV array can be ensured by incorporating a maximum power tracker between the inverter and induction motor. Any suitable scheme of speed control such as constant v/f ratio, constant flux and slip regulation can be employed. There is no published literature on photovoltaic induction motor pump drive. However some manufacturers, like 'GRUNDFOS International Denmark' have designed such drive with 3 phase induction motor, PWM inverter and submersible pump employing constant v/f ratio speed control scheme and maximum power tracker with claimed efficient performance.

### 2.3.3 Synchronous Motor:

The synchronous motor for pumping applications are used either as a true synchronous motor where speed is controlled by an independent oscillator or in self control mode where pulses for firing of stator inverter are obtained from the shaft sensors so that speed of rotation of stator flux is always equal to the speed of rotation of rotor. Self controlled synchronous motor (SCS) is also known as dc commutator less motor due to similarity of operation. For low power applications such as photovoltaic pumping system,

permanent magnet self controlled synchronous motor are preferred due to following advantages [8].

- i) It can be operated at near unity power factor. Elimination of reactive power results in minimal size of inverter - motor system.
- ii) Load commutation is possible. This make the inverter simple, more efficient and reliable, when thyristors are employed.

Therefore permanent magnet self control synchronous motor seems more attractive than the permanent magnet dc motors. Because these motor do not have slip rings or brushes. However electronics gave reliability problems and it is some what less efficient than the better brushed permanent magnet ~~electric~~ d.c. motors [7]. For the low power application power transistors and MOSFET's are employed in the inverter to eliminate forced commutation problems. The speed of the drive can be controlled by keeping v/f ratio constant so that the motor runs under ideal flux condition.

## 2.4 PUMPS

There are two types of pump namely positive displacement and centrifugal. For low heads applications such as small

irrigation pumping system, positive displacement pumps seems inappropriate on efficiency, size and starting consideration. Therefore a simple single stage centrifugal pump seems to be best choice. The UNDP project report recommends for the same. The several approaches have been published in literature to ensure efficient and stable operation of pump. Author [12] suggest a graphical approach to operate the pump at its maximum efficiency with the help of Q-H curves of pump and system. While author [11] suggest an analytical methods for analysis and prediction of performance of the pump. Selection of a centrifugal pump is made so that it fulfills all the requirement of the systems and its base speed Q-H curve should intersect the maximum efficiency point in the system Q-H curve. Then an appropriate drive is selected to match the pumping power requirements at variable speed.

## CHAPTER 3

### PROPOSED DRIVE SCHEME

#### 3.1 INTRODUCTION

The water pumping for irrigation purposes is one of the application of photovoltaic power. Usually time and amount of PV power matches the water demand of irrigation, otherwise excess water during summer can be stored in tanks or reservoir for latter use. This storage technique is more efficient and economical than the battery storage of PV power. The remote location of pumping systems and high cost of PV array suggest the use of a drive, which has high efficiency, high reliability, low cost and needs very little maintenance. Various drive schemes are possible. Some of them were discussed in the previous chapter. The permanent magnet dc motor drive is most efficient but gives maintenance problems. The ac permanent magnet motor drive overcomes the problem of maintenance but involves complicated electronics which may cause problems of reliability. The next alternative is induction motor drive. The only disadvantage of this drive is low efficiency specially in small power applications. For the power level below 500W, single phase induction motors

are preferred due to their easy availability. These motors need ~~smaller~~, less expensive, ~~more reliable~~ and simpler inverter than poly-phase induction motor due to less number of components. The main disadvantage of a single phase induction motor drive is low starting torque. The permanent capacitor motor is preferred because it is free from the fractional parts such as centrifugal, switch or brushes [13]. The efficiency and power factor of permanent capacitor motor is higher than that of other single-phase motors. Due to high power factor the reactive power consumption is less, which results in low RMS current rating of power switches. Moreover, low starting torque does not pose any problem with the parabolic loads such as fan or pump loads. Therefore for a small power PV water pumping system, single phase permanent capacitor induction motor is one of the best suitable choice. Such a drive consists of a PV array module, an induction motor and an inverter with suitable control scheme as shown in Fig. 3.1.1. In this chapter, these components of the drive scheme will be discussed.

### 3.2, PV ARRAY MODULE

The solar cell which converts solar energy directly into the electricity is capable to produce 0.6 - 0.8 of peak watts of power. Usually they are connected in series,

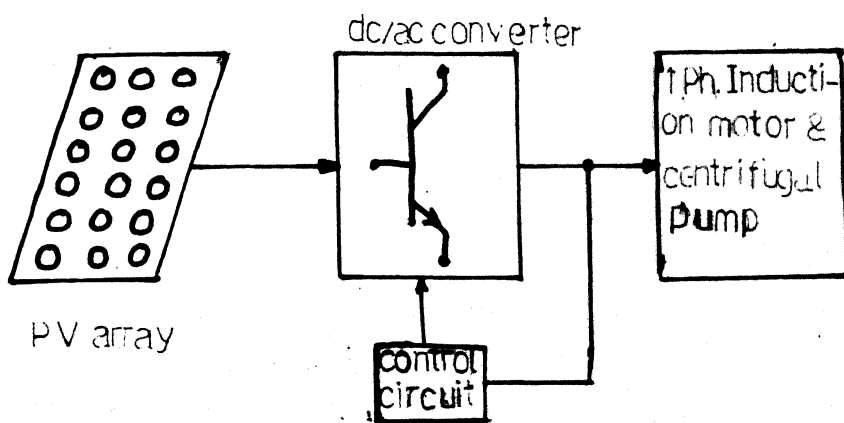


Fig. 3.11 Proposed drive scheme

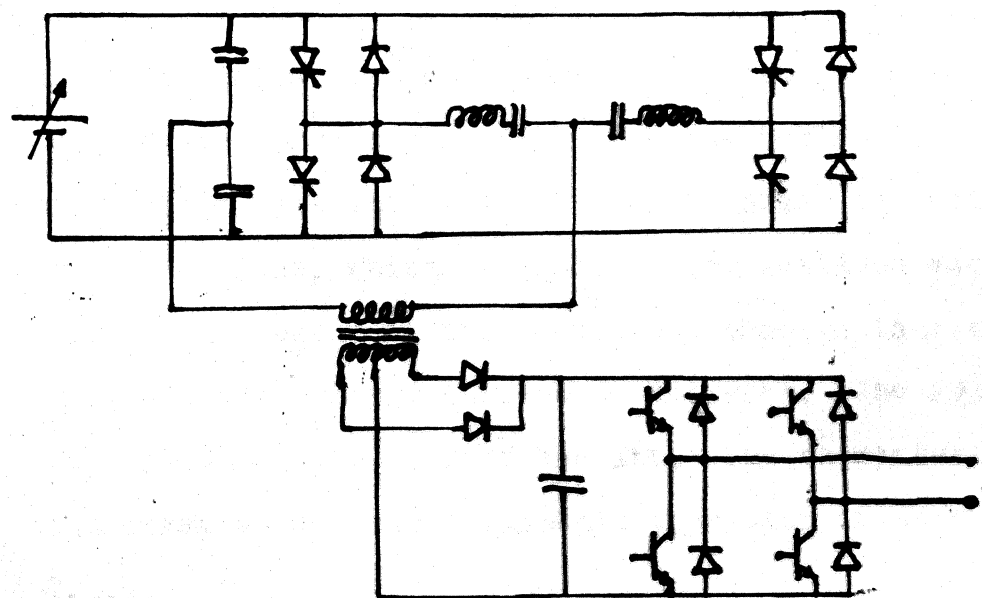


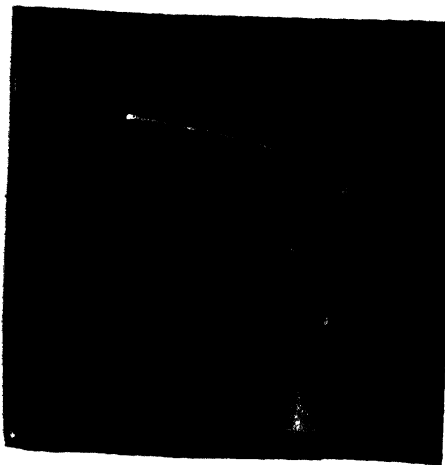
Fig. 3.3(a) High frequency link resonant inverter

parallel or in combination of both to produce the desired input voltage, current. Generally low current high voltage connections are preferred to limit the losses in the load. However a dc voltage greater than 80 volts may present serious electricution hazard and should be avoided. The PV arrays should be mounted on a structure so that they receive optimum solar energy throughout the year and should be protected against the climatic condition of the site.

A PV array module was designed by connecting four solar cell pannels in series. Each pannel contains 36 series connected solar cells to produce 25 watts of peak power. These pannels were mounted on an iron frame facing south. The frame was bolted to a structure so that it makes an angle of  $26.44^{\circ}$  from the plane, which is equal to the latitude angle of the site. This value of tilt angle was choosen to receive optimum solar energy throughout the year. The PV array module was placed on the roof of the lab. The characteristics of the array at a typical climatic condition is shown in Fig. 3.2.1.

### 3.3 INVERTER

The photovoltaic induction motor pump drive needs a static inverter to convert available direct current PV power



scale :-

vertical axis -

PV current (1.66 A / div.)

horizontal axis -

PV voltage (10 V/div)

Fig. 3.2.1 Oscilloscope showing characteristics of PV array

into ac power. The static inverter uses power semiconductor switches which are operated at desired frequency to produce alternating current. Such an inverter should produce a sinusoidal current, with low harmonic ~~and the switch~~ should operate <sup>at high frequency</sup> over a large range of input power and voltages. The reliability of the circuit is also important and can be improved by using least possible number of components. The most commonly used power switches are thyristors (SCR) due to their low cost in high power ratings. But they require <sup>for Comm. to Z</sup> an auxiliary devices which affects the efficiency and reliability of the inverter. Development of the self extinguishing devices such as Gate Turn Off thyristors (GTO's), Power Transistors and Metal Oxide Field Effect Transistors (MOSFETs) have made it possible to realize reliable forced commutated inverters operated at high frequency. Such inverters have high efficiency, low total harmonic distortion in the output less volume and weight in comparision of conventional thyristor inverters. In the low power and medium frequency applications, power transistors are prefered due to low conduction and switching losses.

The various circuits are reported for use in the photo-voltaic application such as high frequency link inverters [5,14]

and high efficiency inverter [6]. The high frequency link inverter are commonly used in residential photovoltaic power conditioning system where the ~~main~~ <sup>↓</sup> considerations are less weight, volume and total harmonic distortion in the output. In such an inverter dc power is converted into high frequency ac, which is then ~~transfor~~<sup>coupled</sup> and converted ~~in~~ to the required frequency ac through a dc link ac to ac converter as shown in Fig. 3.3.1. The multistage in the conversion results is low efficiency, low reliability and high cost. Author [6] has reported a simple inverter which converts dc PV voltage into constant frequency ac voltage without an intermediate dc link, as shown in Fig. 3.2.2 which results in good efficiency and reliability. An inverter was designed and fabricated with less number of components than that of Fig. 3.3.2. The new inverter needs only three power switches, a flywheeling diode and a central tap transformer. The circuit of inverter without protection and control circuit with waveform at different points is shown in Fig. 3.3.3.

The main power switch MT is operated at high frequency (20 KHz) employing PWM techniques as a <sup>U</sup> converter, which produces a pulse width modulated high frequency current,  $I_1$

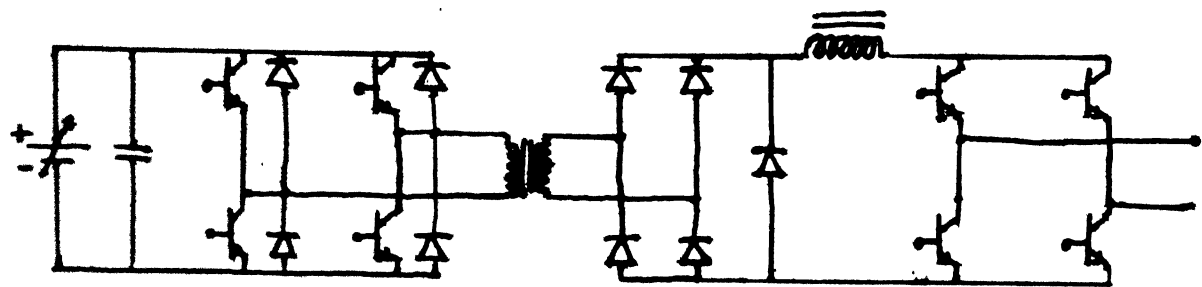


Fig. 3.3.1a High frequency link inverter

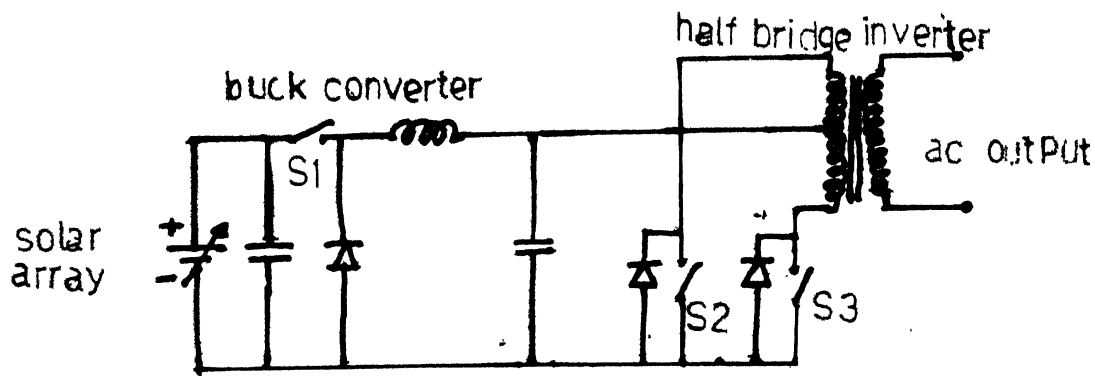


Fig. 3.3.2 Single stage inverter

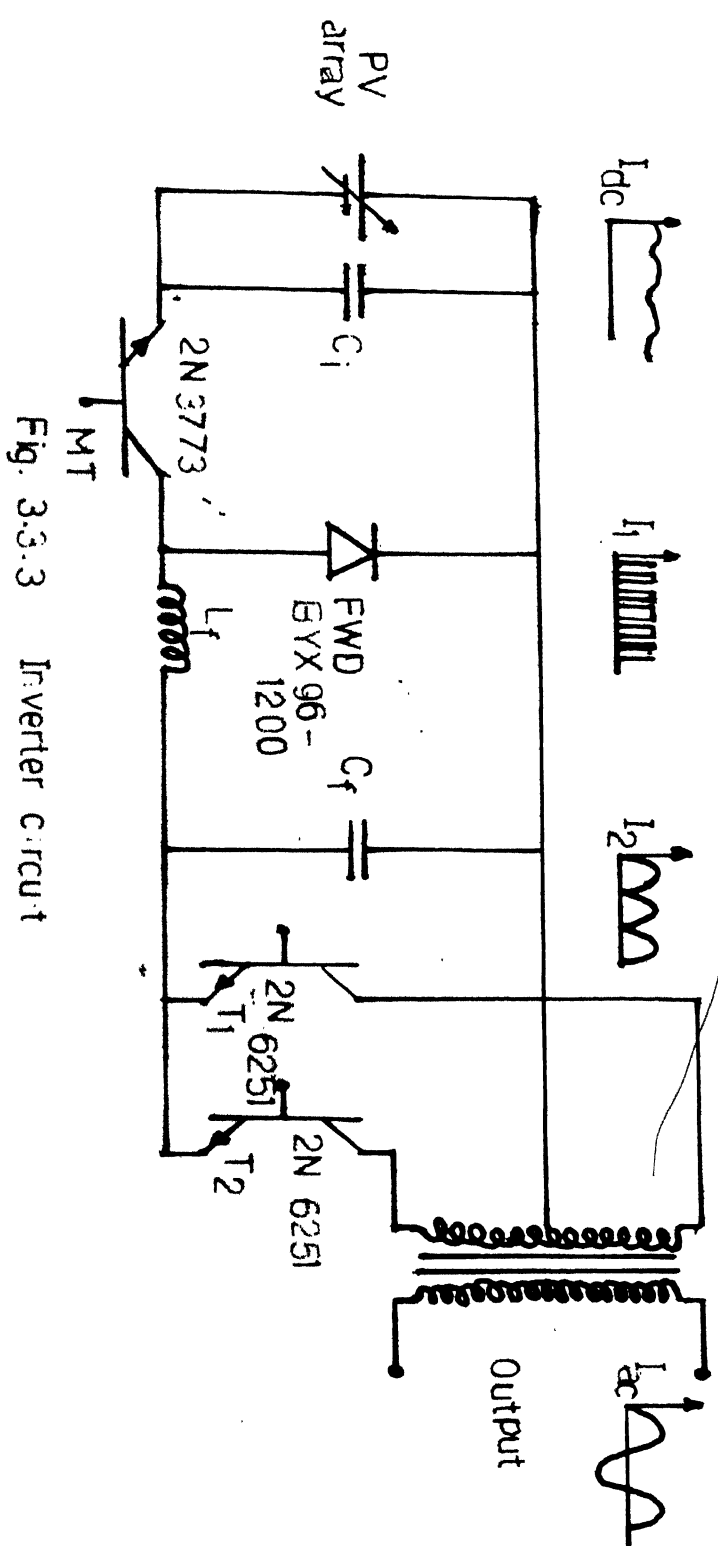


Fig. 3.3.3 Inverter circuit

from the variable PV current  $I_{dc}$ . This rectified sinusoidal current  $I_2$ . The power switches  $T_1$  and  $T_2$  form a half bridge polarity reversing inverter with transformer. The  $T_1$  and  $T_2$  are operated at desired frequency to produce a sinusoidal ac current  $I_{ac}$  at the output. The transformer is used to prevent the flow of dc current into the motor and to isolate PV array from the motor. A capacitive filter is connected at the input to limit the ripples in the input voltage and current. A flywheeling diode  $D_1$  is connected to provide an alternative path for the current during the off period of MT.

All three power switches were <sup>year</sup> realised by power transistors (2N3773). The high frequency (20 KHz) of the chopper was chosen in order to obtain small filtering components ( $L_f$  and  $C_f$ ) and low switching and filtering losses. The low pass filter was realised by a metalized paper capacitor  $C_f$ , (15  $\mu$ F) connected in series with an air core inductor  $L_f$  (135  $\mu$ H). The flywheeling diode uses a fast recovery diode (BYX96). The input filter was realized by a parallel combination of metalized paper capacitor (15  $\mu$ F) with a electrolytic capacitor (2200  $\mu$ F) to store high frequency <sup>and</sup> low frequency components respectively. A central tap transformer was designed with turn ratio 1:5.5 to produce the desired output voltage level.

### 3.4 CONTROL SCHEME

The development of the solid state power controllers made it possible to operate the drive in the desired manner. The power output of the drive can be optimized by employing a suitable control scheme. In conventional power fed pump drive, control scheme is responsible for stable and efficient operation of drive, thereby ensuring optimum mechanical output (water). But in case of photovoltaic pump drive, the control scheme should not only be responsible for maximum mechanical output but also the maximum conversion efficiency of PV arrays. An increase in the conversion efficiency reduces the required solar cells arrays area which will result in considerable reduction of overall cost of the drive. The cost of the PV array is more than 80% of the total cost of the drive. In photovoltaic induction motor pump drive, there are two possible control variables, modulation index and frequency <sup>↓</sup> of the output of inverter. These variables can be controlled in two ways.

- 1) select an optimum operating point of the motor characterised by input current and frequency. The motor will absorb a certain power which thus characterised an operating point of photovoltaic array,

ii) operate the PV array at its optimum power which imposes the supplied power on the motor. This leads to a search for a frequency of input supply which guarantees an optimum efficiency from the motor.

Therefore such a drive has two degree of freedom, modulation index  $m$  of the inverter, which controls the PV array operation point at optimum power and frequency of inverter output  $f$ , which optimises motor efficiency. The second control ~~will~~ will ensure the optimum power input to the motor only if the efficiency of the inverter is independent of the load current which is rarely the case. Therefore first control scheme is more preferable. This scheme was implemented in proposed drive.

### 3.4.1 Control of Modulation Index:

The amount of the photovoltaic output power entirely depends upon the location of the operating point of the system on IV characteristics of solar cells array. The operating point of the system is the intersection point of the IV characteristic of the array and the load line as shown in Fig. 3.4.1. Since the IV characteristic of the solar cell array has a fixed size and shape for a particular values of temperature and insolation level, the location of the operating point is mainly decided by the slope of load line.

Therefore amount of the output power of a solar cells array can be controlled by changing the slope of load line and hence can be maximised by adjusting the slope of load line so that operating point of the system concides maximum power point of the PV array. The slope of load line depends upon voltage and current level of the load ( $\frac{V}{I}$ ) and hence can be controlled by changing the modulation index of the inverter. Thus proper adjustment of the modulation index can ensure the maximum output power from a PV array. This can be done by sampling the output power of array and changing the modulation index 'm' of the inverter until the power is maximised. The power output of the PV array can be sampled simply by multiplying the voltage and current reading together. This will involve a large number of multiplication and sensing of both voltage and current, which need a microcomputer. The several maximum power tracker are reported in the literature [5,6] for the residential power conditioning system which work on the above principle and use a single chip microcomputer. However, for the photovoltaic pump drive which is to be located in remote sites the use of microcomputer is risky and reliable operation of such a system is doubtful in field conditions.

The power output of the PV array can also be maximised by maximising the <sup>input</sup> voltage or current input to the load provided I-V characteristic of the load does not reaches a maximum. In other words load line does not have a negative slope region which can be true in case of induction <sup>motor</sup> pump drive if proper speed control scheme is employed. In the proposed scheme the input voltage to the motor is sampled regularly and modulation index is varied. If the input voltage to the motor increased or remain same the modulation index is varied in the same direction otherwise direction of change in the modulation index is reversed. Thus the operating point of the system fluctuates around the maximum power point of the PV array. The actual circuit used and its operation will be discussed in the next chapter.

### 3.4.2 Control of the Frequency:

The control of the modulation index will ensure the optimum voltage input to the motor. Since the mechanical output power of pump drive is proportional to the speed, a suitable speed control scheme should be employed which adjust the speed of the drive for corresponding change in the input voltage. Usually speed of the single phase permanent capacitor motor is controlled by reducing the strength

of the air gap magnetic flux or the synchronous speed of the motor. The strength of the magnetic flux can be controlled by changing the stator voltage at constant frequency, while synchronous speed of the motor is controlled by varying the frequency of the stator supply.

The speed-torque characteristic of a single phase permanent capacitor motor for different stator voltage is shown in Fig. 3.4.2a. This method of speed control is most suitable for the parabolic load such as pump because of ~~limited~~ large range of speed control. The disadvantage of this method is low efficiency at low-speed range. Moreover the input current of the motor increases with decrease in the speed upto about 33% slip and then start decreasing. Therefore the load line will have a negative slope if the slip of motor is more than 33% which is undesirable for the proposed maximum power tracking scheme.

The other way of speed control is by controlling the input frequency. The voltage ~~is~~ to the frequency is in ~~ratio~~ ~~kept~~ ~~depth~~ constant to ensure the operation of motor at ideal flux condition. In poly-phase induction motor the constant maximum torque is produced at all speeds. But in the single phase induction motor, this is not the case. The maximum

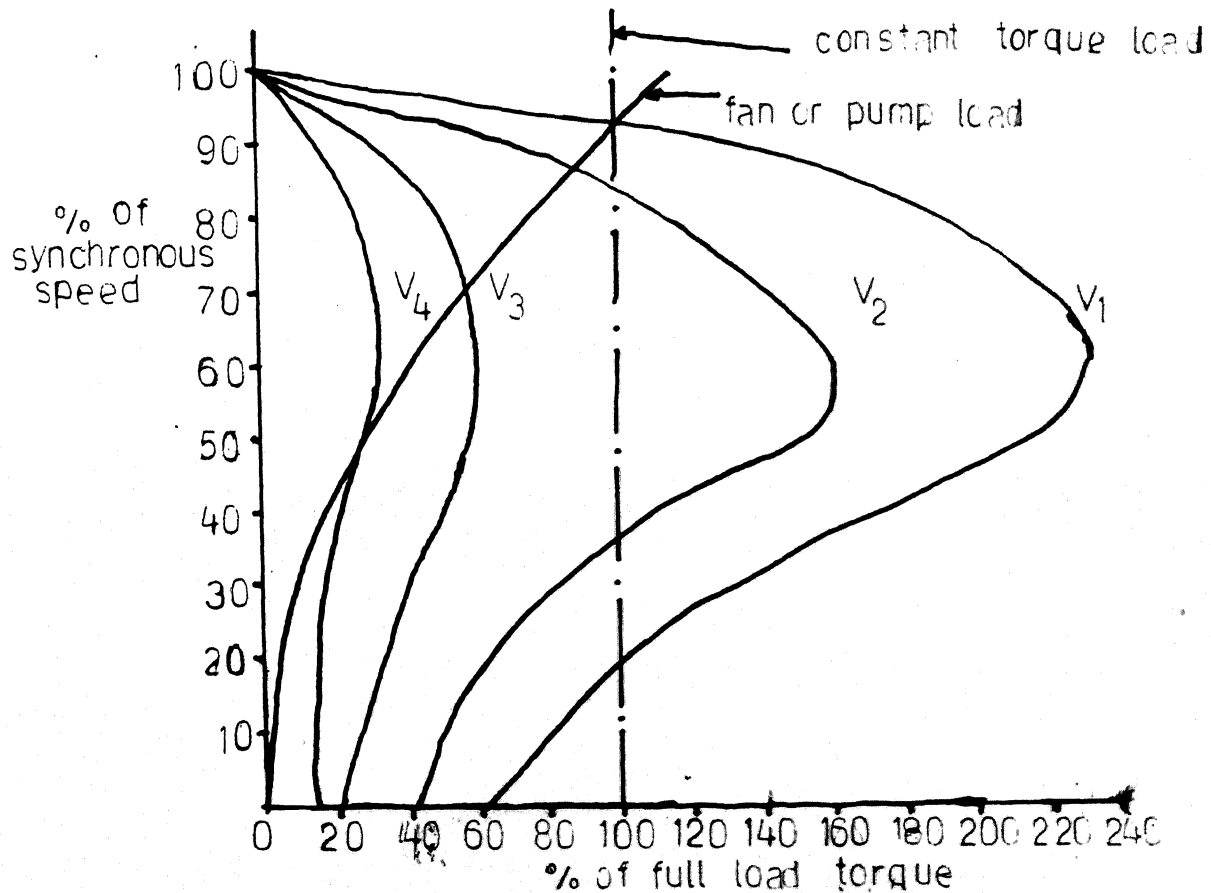


Fig. 3.4.2a Speed-torque characteristics of permanent capacitor I.M. with variable Voltage

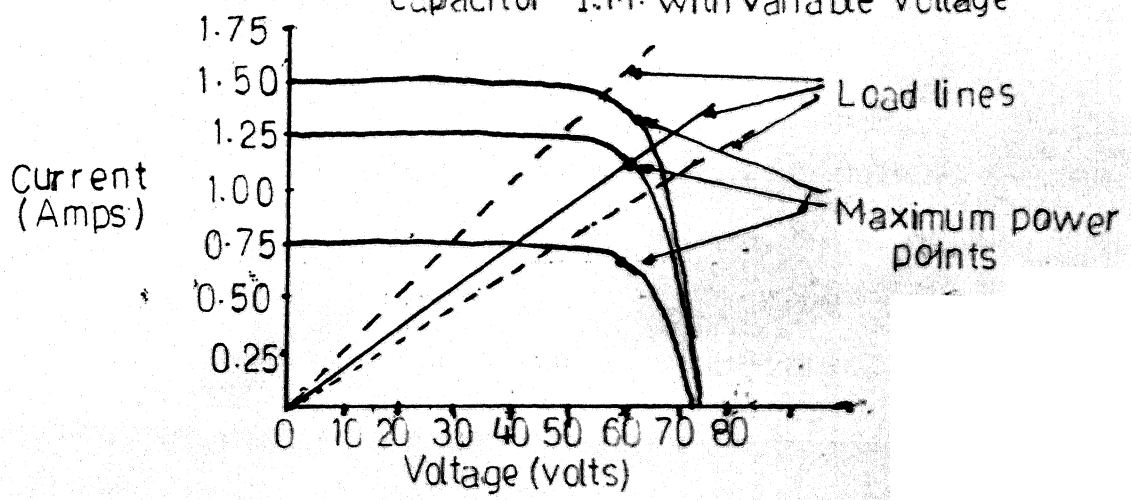


Fig. 3.4.1 PV array characteristics & load line

torque produced by the motor decreases with the decrease in the speed inspite of constant V/F ratio as shown in Fig. 3.4.2b.

The reason is quite simple. The strength of the cross magnetic flux in the single phase induction motor depends upon the speed voltage induced in the rotor and decreases with the speed. The reduction in the torque at low speed is favourable for pump <sup>and</sup> fan loads. This method of speed control is more efficient than the former one. The efficiency of drive can be improved further by varying the V/F ratio so that the maximum torque produced by the motor is slightly more than the load torque at all speeds.

In this project both of the speed control schemes were implemented.

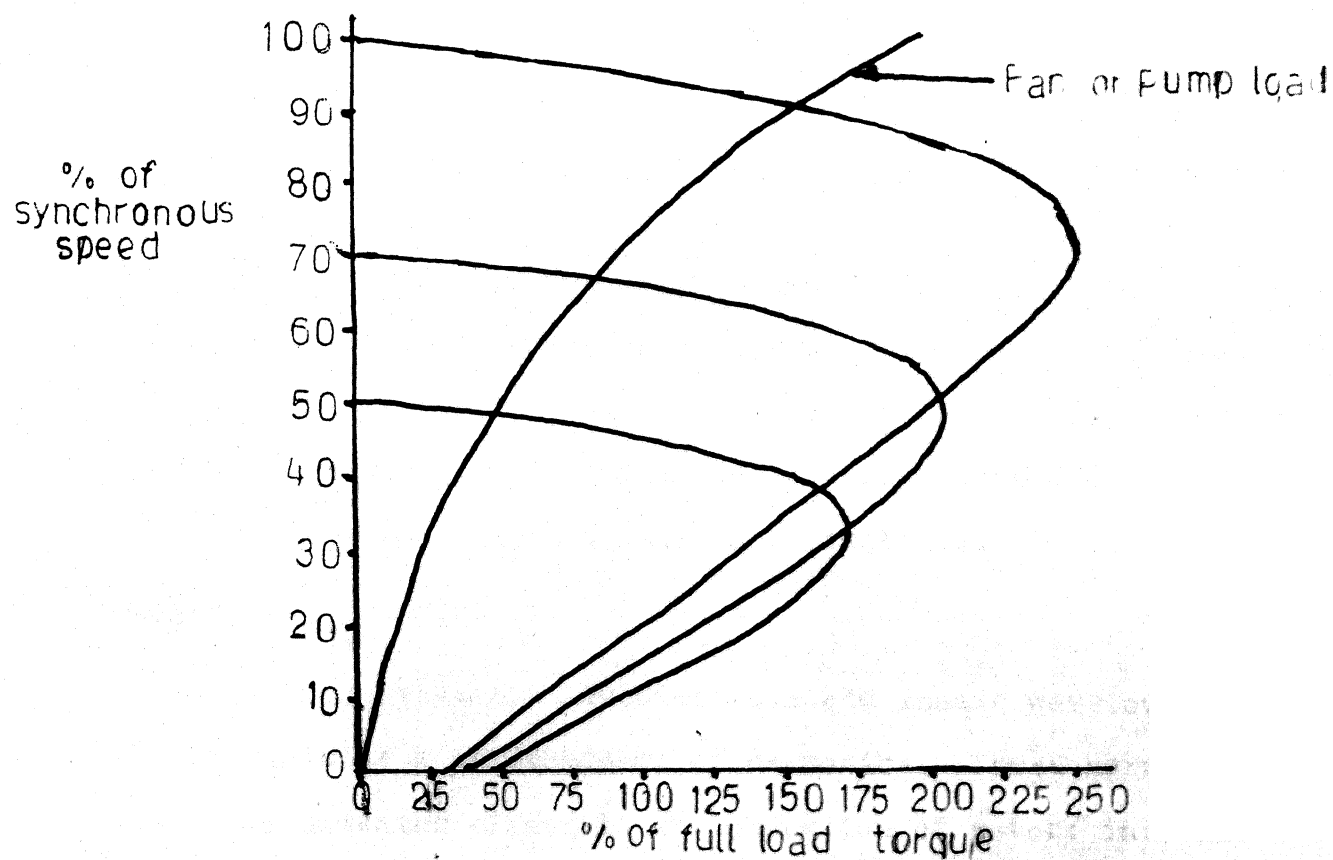


Fig. 3.42b Speed-torque characteristics of permanent capacitor I.M. with constant V/f ratio

## CHAPTER 4

### CONTROL AND PROTECTION CIRCUITS

The design and operation of the control and protection circuits will be discussed in this chapter. The control circuit consists of firing circuit, base drive circuit, maximum power tracker circuit and voltage controlled oscillator (Fig. 4.1), while snubbers <sup>ave</sup> were provided to protect the power switch from secondary breakdown. Since the PV array regulates its voltage and current, no protection is provided for over current or over voltage to the power switches.

#### 4.1 FIRING CIRCUIT

Normally static inverters produce square wave output, which contains a large number of harmonics. These harmonics have two unwanted effects, in the operation of motor, increase in heating and torque pulsation due to distortion in the air gap flux. Therefore, it is desirable that harmonic components of the waveform should be minimum. The harmonic content of the waveform can be controlled by employing pulse width modulation techniques. There are several PWM techniques such as sinusoidal PWM modulation with uniform sampling (SPWM) optimal PWM and harmonic elimination. For the transistor inverters

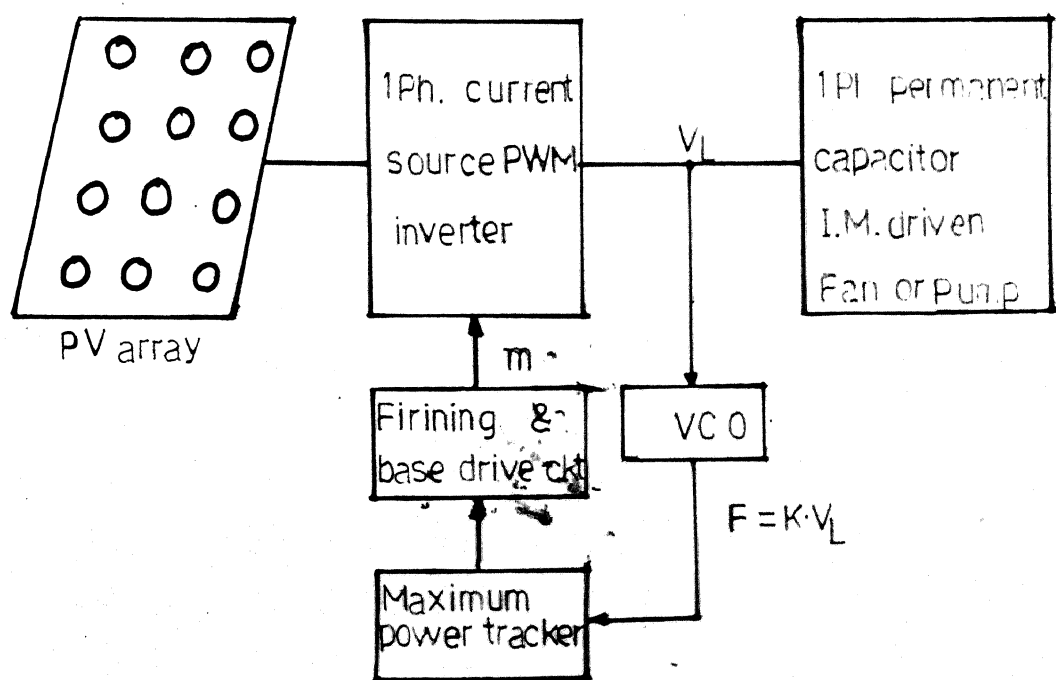


Fig. 4.1 PV Induction motor pump drive

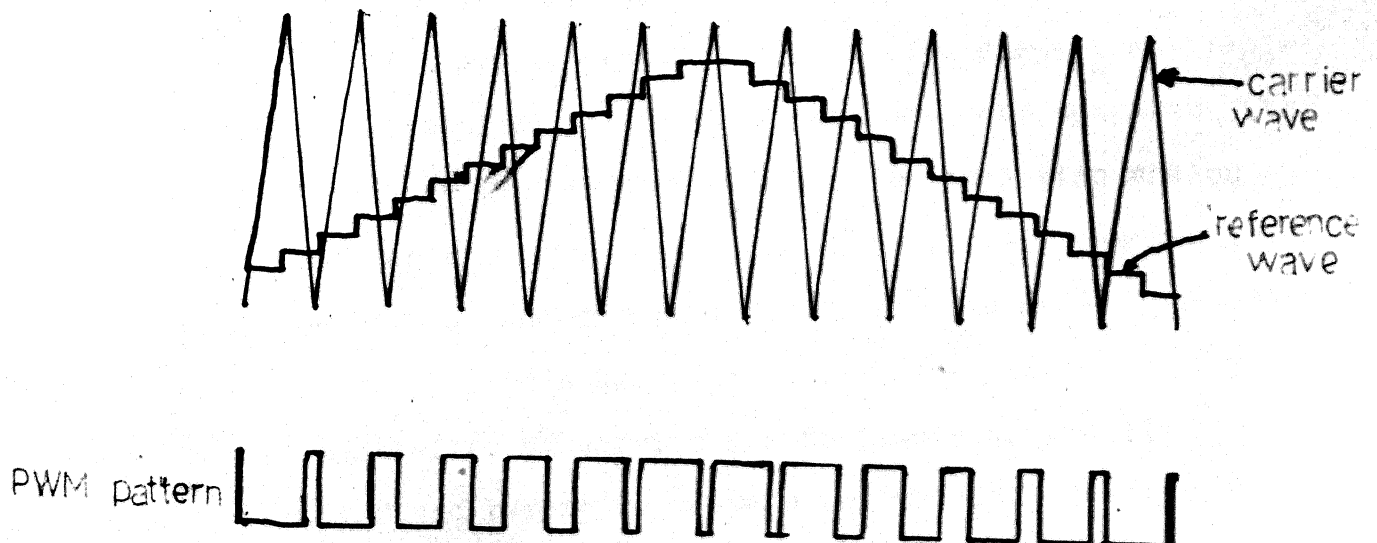


Fig. 4.1.1 PWM pattern generation

SPWM is most suitable and can be implemented either by natural comparision. In natural comparision a sine wave of variable frequency and amplitude is compared with the triangular wave of carrier frequency. Since it is difficult to generate a sine wave of variable frequency and amplitude, the author of reference [7] have used trapezoidal reference wave instead of the sinusoidal. The switching instant can be calculated on main frame computer and can be stored in EPROM. However for high carrier frequency a large storage area will be required, which is not economical.

In the proposed drive scheme a stepped triangular reference wave of variable frequency and amplitude was used because it is easy to generate such a wave shape than trapezoidal or sinusoidal. This reference wave was compared with fixed frequency (20 KHz) triangular wave employing analog techniquea as shown in Fig. 4.1.1. The circuit was realised with the help of the counters and digital to analog converter (DAC). The amplitude and frequency of the reference wave can be controlled by varying the frequency of the clock for the counter and reference voltage of the DAC1 respectively. The clock is provided either by an independent oscillator, - whose frequency can be controlled or from the output of a VCO.

The independent oscillator <sup>is</sup> realized by NE566 chip. The output frequency is kept 1024 times the desired output frequency. The magnitude of the reference voltage to the DAC is provided from the output of maximum power tracker circuit. The complete circuit is shown in Fig. 4.1.2 and its waveform is Fig. 4.1.3.

A 8 bit up down counter, which uses two cascaded 74191 chips, counts the input clock continuously and produces a high pulse CO at max./min. pin, whenever its count content becomes 00 or FF. The signal CO triggers a positive edge ~~more~~ MV [1/2 74LS221] to produce a short duration pulse (2  $\mu$ sec). This pulse toggles a JK flipflop [1/2 7476] to produce a signal U. The signal U is connected to the up down pin of the counter which makes the counter to count up and down when its content becomes 00 and FF respectively. The counts output of the counter is connected to digital to analog converter [ADC 7523JN]. The output of DAC is level shifted and amplified to produce the stepped triangular reference wave RW. The fixed frequency triangular wave is generated by using a NE<sup>S</sup>66 timer. The output of timer is level shifted and amplified to produce carrier wave CW. These waves RW and CW are compared by using a high speed comparator [LM361], whose

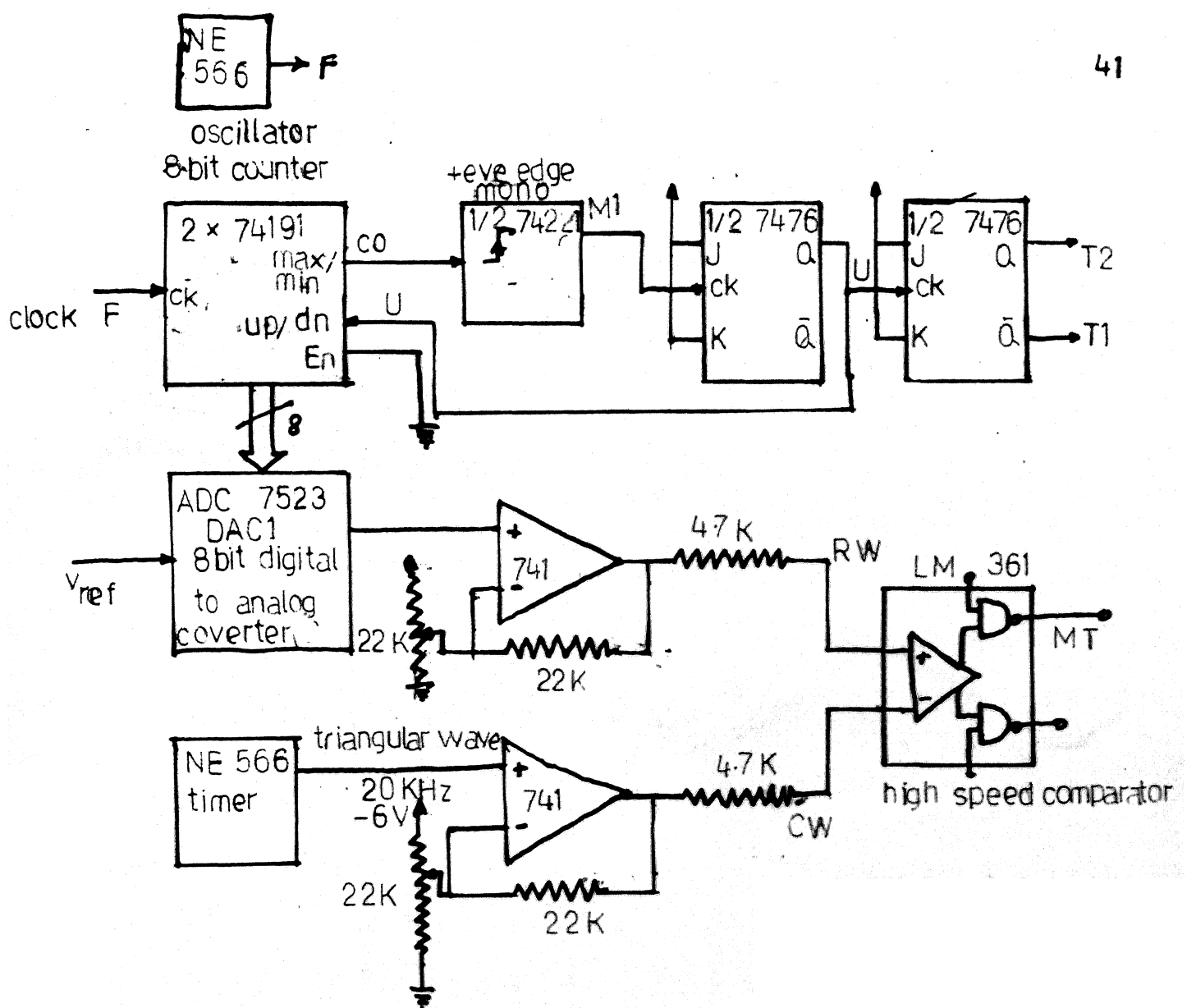


Fig. 4.1.2 Firing circuit

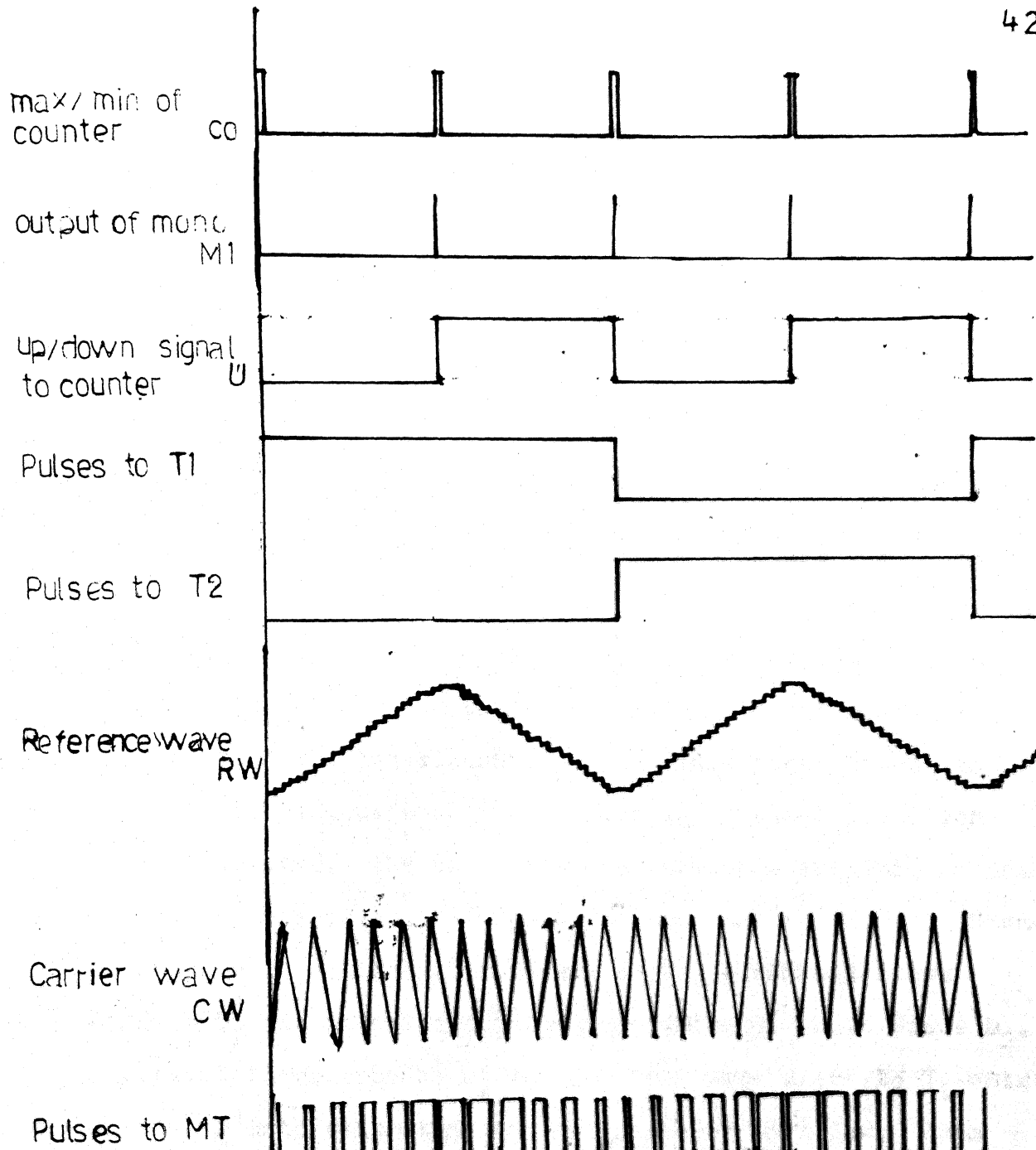


Fig. 4.1.3 Waveforms at different points of firing ckt.

output is the required PWM pattern. The signal toggles an another JK FF [1/2 7476] to produce the complemented square waves. The frequency of these waves is half of the frequency of reference wave and used to trigger power transistor  $T_1$  and  $T_2$ .

#### 4.2 BASE DRIVE

The base drive circuit is used to amplify the switching pulses and to reduce the switching time and conduction losses. The firing circuit should also be protected from the high speed large voltage and current transient in the power circuit by isolating the two circuits [16]. Since power transistor requires continuous base drive, pulse transformer isolation can not be used. The opto isolator are used for this purpose, such an optoisolator 4370/5082 is shown in Fig. 4.2.1. Whenever there is a high pulse at the input, a current flows through  $D_1$  and it emits light which strike to photo diode  $D_2$ . A current flows through  $D_1$  and provides base drive to  $T_1$  which drives  $T_2$  into saturation and hence output goes low. When input signal is low  $T_2$  will be in cut off and output will be high. The optoisolator needs an isolated power supply to ~~isolate~~ the output from the input. Such a power supply was designed as shown in Fig. 4.2.2.

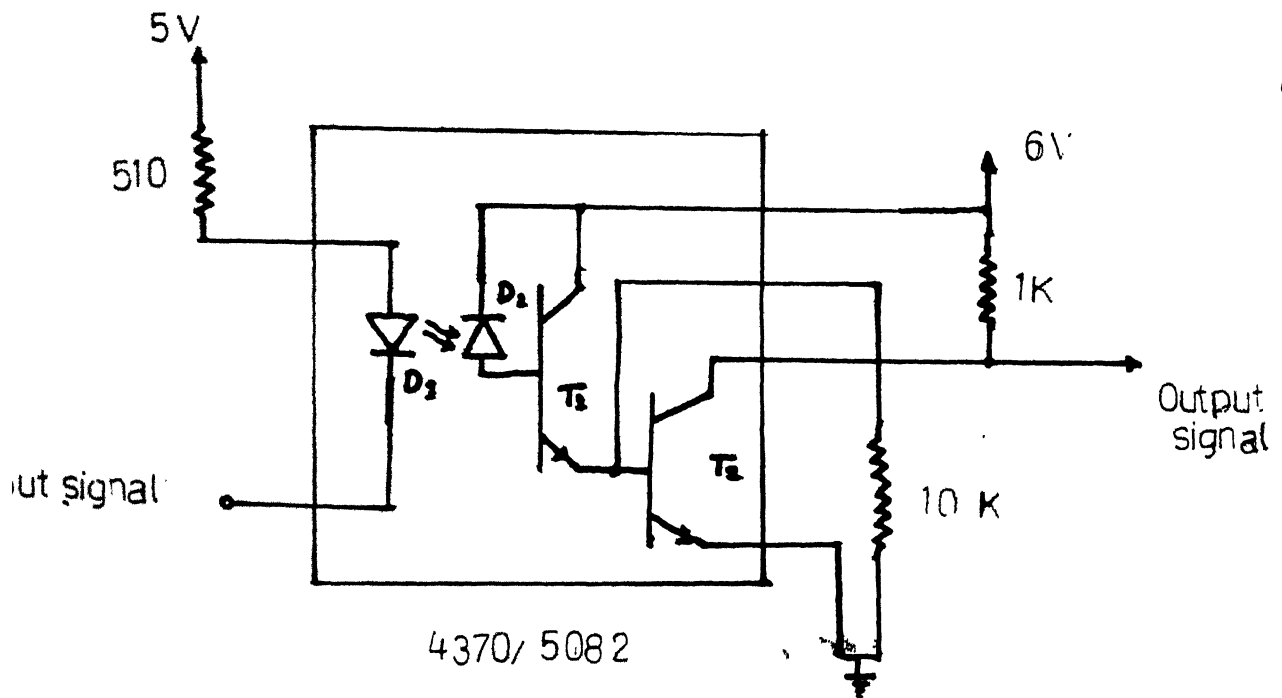


Fig. 4.2.1 Optical isolator

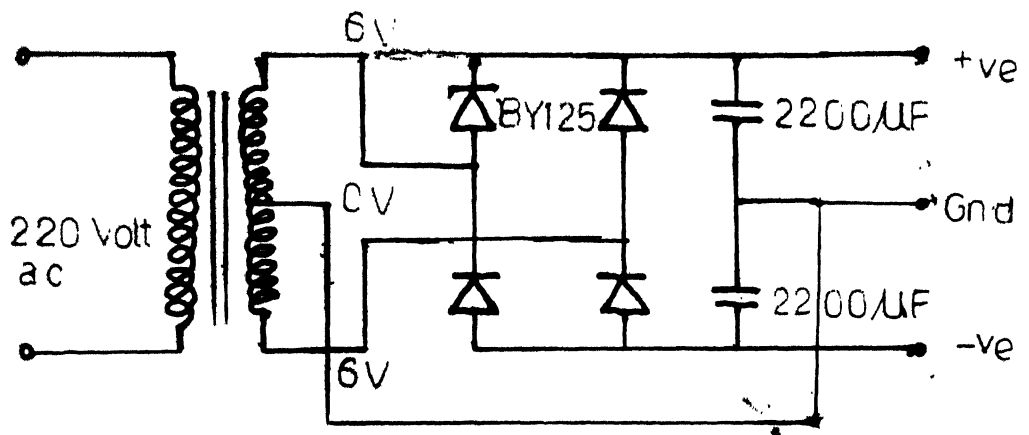


Fig. 4.2.2 Isolated power supply

A simple base drive circuit was realised as shown in Fig. 4.2.3. Input signal is isolated and amplified by transistors  $Q_1$  and  $Q_2$  so that it can drive transistor pair  $Q_3-Q_4$  into saturation. To reduce the storage time and hence the switching time and losses, transistor,  $Q_4$  produces the negative base drive when power transistor is to be off. An alternative path for the negative base drive is provided by connecting zenor diodes <sup>and</sup> at the output after the storage time, which protects the base emitter junction from the avalanche breakdown. The storage time can be reduced further by controlling the depth of the saturation of the PT. This was obtained by connecting diode  $D_1$ . As the saturation level of PT  $\frac{1}{2}T$  increases,  $D_1$  becomes forward biased and by passes certain portion of the base drive of  $Q_3$  <sup>and</sup> to collector of the PT and hence reduces the base drive to the PT and thus reduces the saturation level. The capacitors, in the collectors circuits of  $Q_3$  and  $Q_4$  are connected to provide high initial base drive of about 2.5  $\mu$ sec.

#### 4.3 VOLTAGE CONTROLLED OSCILLATOR

The circuit of VCO is shown in Fig. 4.3.1. The input voltage to the motor is stepped down, rectified and filtered to obtain a dc voltage  $V_1$ . The dc voltage  $V_1$  is proportional to the motor terminal voltage and connected to control voltage

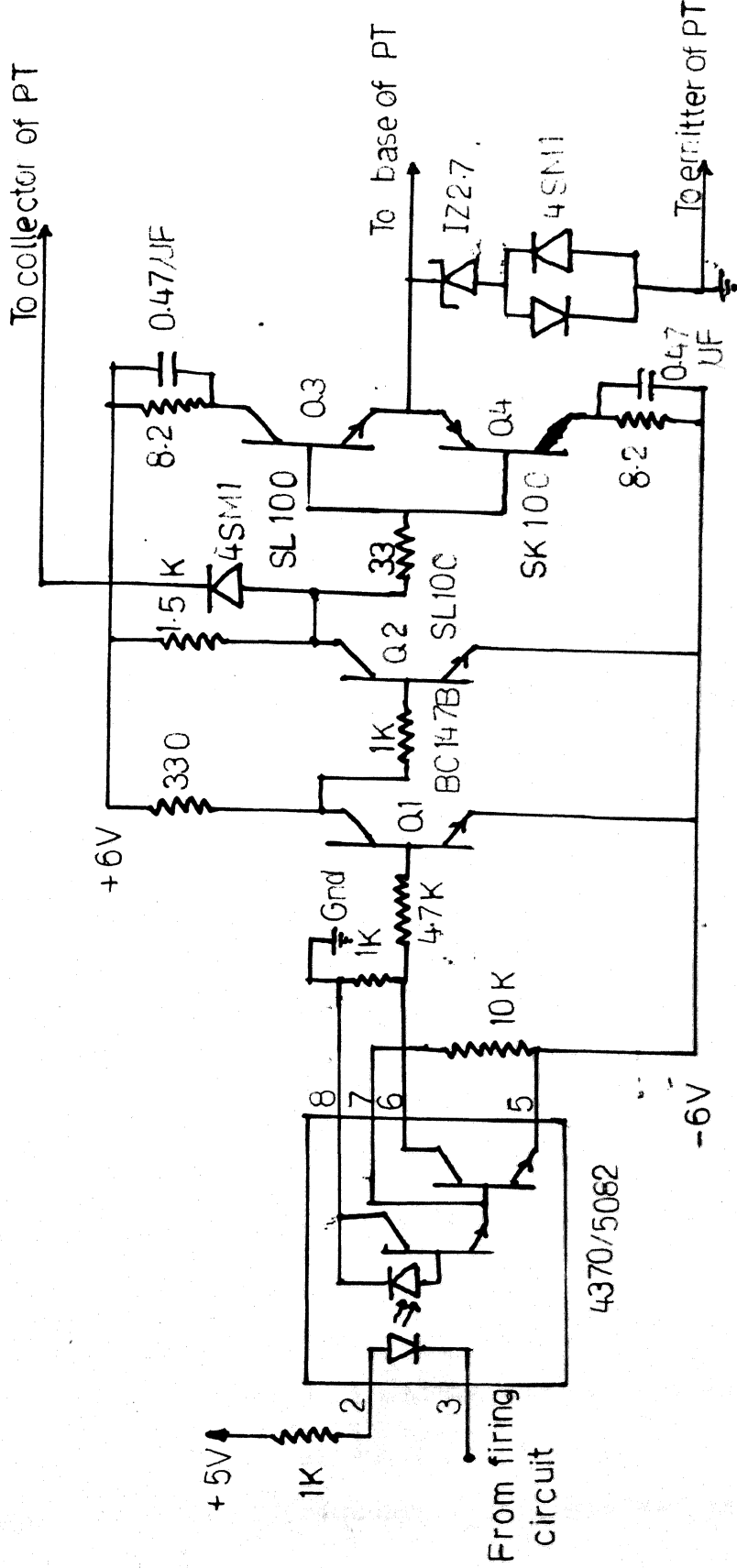


Fig. 4.2.3 Base drive circuit

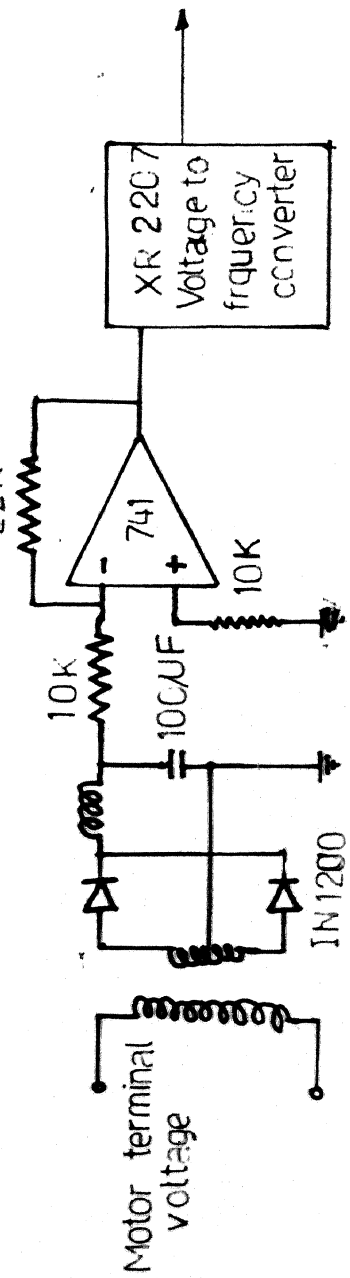


Fig. 4.3.1 VCO Circuit

pin of a voltage to frequency converter chip [XR2207]. The timing components of XR2207 chip is selected to maintain a constant ratio of its output frequency to motor terminal voltage so that the ratio of the motor terminal voltage and inverter frequency is maintained at rated value. The rated V/F ratio of motor is 4.4.

#### 4.4 MAXIMUM POWER TRACKER CIRCUIT

A simple maximum power tracker is proposed which maximises the input voltage to the motor by controlling the modulation index of the inverter. The input voltage to the motor is continuously monitored and converted in to frequency by using a VCO. The output frequency of VCO is proportional to the motor terminal voltage ( $V_L$ ). This frequency  $F_1$  is measured and is stored. Then the modulation index of the inverter is either incremented or decremented depending upon the previous condition. The variation in modulation index will change the terminal voltage of the motor and hence output frequency of the VCO will change. An adequate time is provided to settle the power transient. The <sup>new</sup> output frequency of VCO  $F_2$  is measured and compared with the previous value of frequency  $F_1$ . There are three possibilities.

- a)  $F_2 > F_1$  i.e. motor terminal voltage has increased
- b)  $F_2 = F_1$  i.e. the terminal voltage of the motor remains the same
- c)  $F_2 < F_1$  i.e. the terminal voltage of the motor ~~is~~ has decreased.

In cases (a) and (b), since the motor terminal voltage is either increased or remain the same, the change in the value of modulation index is considered in right direction and it will be maintained in the next cycle. While in case (c), the terminal voltage is decreased. Therefore change in modulation is considered in the wrong direction, therefore in the next cycle, the direction of the change in modulation index is reversed. The circuit is realised using a digital logic circuit and is shown in Fig. 2.4.1.

The base signal to the power switch  $T_1/T_2$  is used to toggle a JK flipflop  $J_1$  [ $1/2, 7476$ ] which produces a signal A at its Q output. The signal A toggles a JK flipflop  $J_2$  [ $1/2, 7476$ ] and produces  $UD$  and  $\overline{UD}$ . The signal  $\overline{UD}$  is connected to the up/down pin of the 8 bit counter  $C_1$  ( $2 \times 74191$ ). Therefore mode of the counting of counter  $C_1$  changes up and down for every two cycles of the motor terminal voltage. A +Ve edge

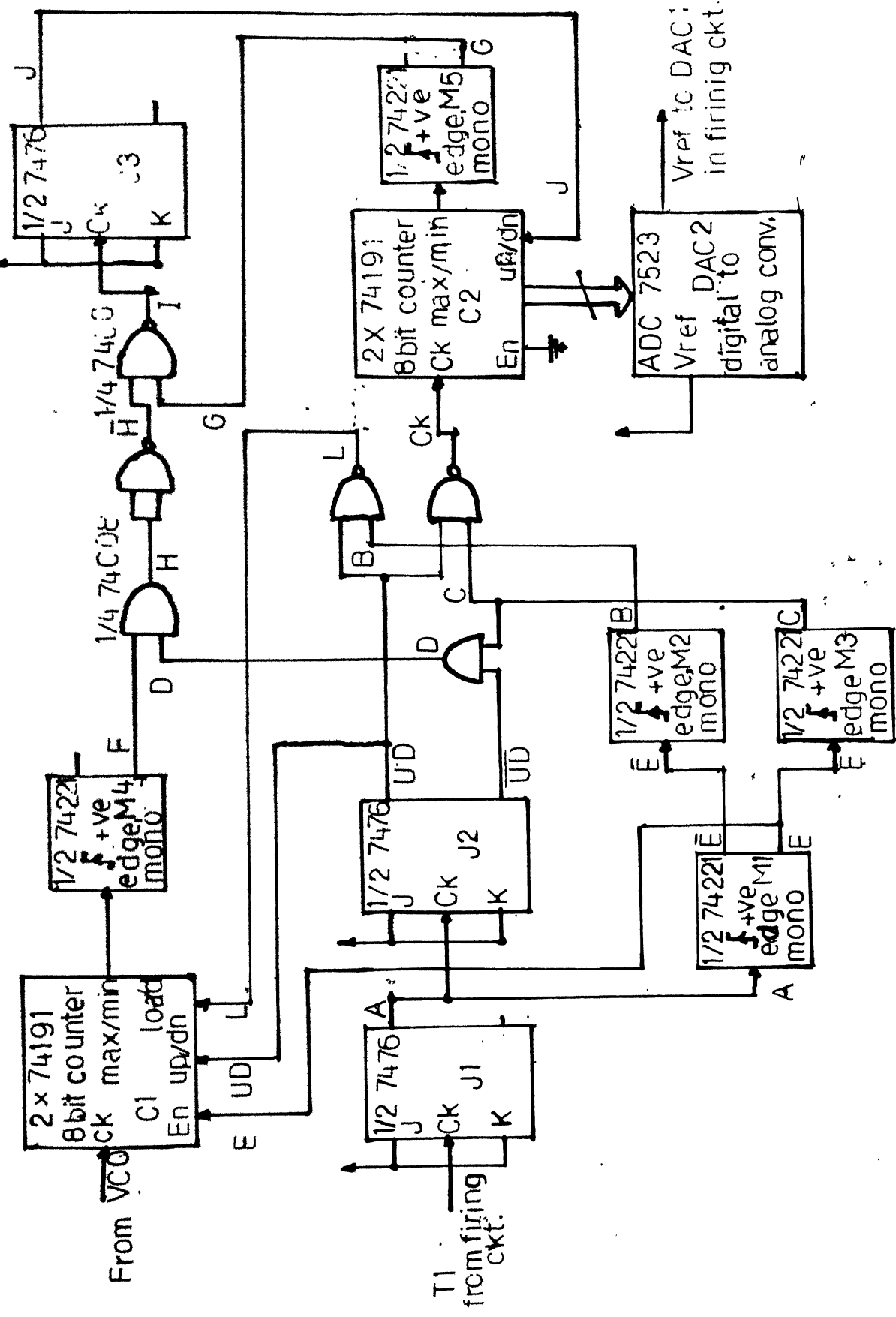


Fig. 4.4.1 Maximum un. power tracker circuit

mono MV  $M_1$  [ $1/2$ , 74LS221] is used to produce a low pulse of 3.8 msec duration at the rising edge of the signal A and is connected to the enable pin of the counter  $C_1$ . This enables the counter  $C_1$  to count up and down alternately for a duration of 3.8 msec. The signal E and T trigger +Ve edge mono MV  $M_2$  and  $M_3$  [7425221] to produce positive pulses B and I of 0.75 and 1.5  $\mu$ sec duration respectively. The pulse B is Nanded with signal  $U_D$  to produce a low level load pulse for counter  $C_1$  so that the counter is loaded with word FF before it starts counting down. The clock to the counter  $C_1$  is provided by the output of the VCO. The output frequency of which is proportional to the terminal voltage of the motor. The pulse C is Nanded with  $U_D$  signal to produce a clock pulse to the counter  $C_2$  (2x74191) whenever counter  $C_1$  stops counting down. The +Ve edge mono MV  $M_4$  [ $1/2$  74LS221] produces a 3.8 msec low level pulse F at the rising edge of ripple clock output of the counter  $C_1$ . The pulse C is Nanded with signal  $\overline{U_D}$  to produce a positive pulse of 1.5  $\mu$ sec whenever counter  $C_1$  stops up counting. The pulses D and F are Nanded together and produce a positive pulse H whenever the counts output of counter  $C_1$  in up counting is <sup>less</sup> than that in down counting. The max./min. output of counter  $C_2$  triggers a +Ve edge Mono MV  $M_5$  [ $1/2$  74LS221], which produces a

negative pulses G of  $1.5 \mu\text{sec}$ . The pulses G and  $\bar{H}$  are Nanded together and produce a signal I which toggels a JK flipflop  $J_3$ . The output of  $J_3$  is connected to the Up-down pin of the counter  $C_2$ . Therefore mode of counting of the counter  $C_2$  changes whenever counts output of counter  $C_1$  in up counting is more than that of down counting or the count output of counter  $C_2$  becomes FF or 00. The counts output of counter  $C_2$  are connected to a digital to analog converter DAC2 [ADC 7523], which produces an analog signal  $V_{\text{ref}}$ . The signal  $V_{\text{ref}}$  is connected to DAC1 in <sup>n</sup>firing circuit. The wave forms are shown in fig. 4.4.2.

The cycle of the operation begins with loading a word  $W$  into counter  $C_1$ . Then counter  $C_1$  starts counting down the output frequency of the VCO for a period of 3.8 msec. At the end of this counting period a clock pulse is released to counter  $C_2$ . The content of the counter is either incremented or decremented depending upon the counting mode of counter  $C_2$ . This will result in corresponding change of the  $V_{\text{ref}}$  signal to DAC1 in firing circuit and hence modulation index will be changed. The circuit remains idle for rest of the two cycles of the terminal voltage of the motor to settle the power transient. Then the counter  $C_1$  starts counting down the output <sup>UP</sup>

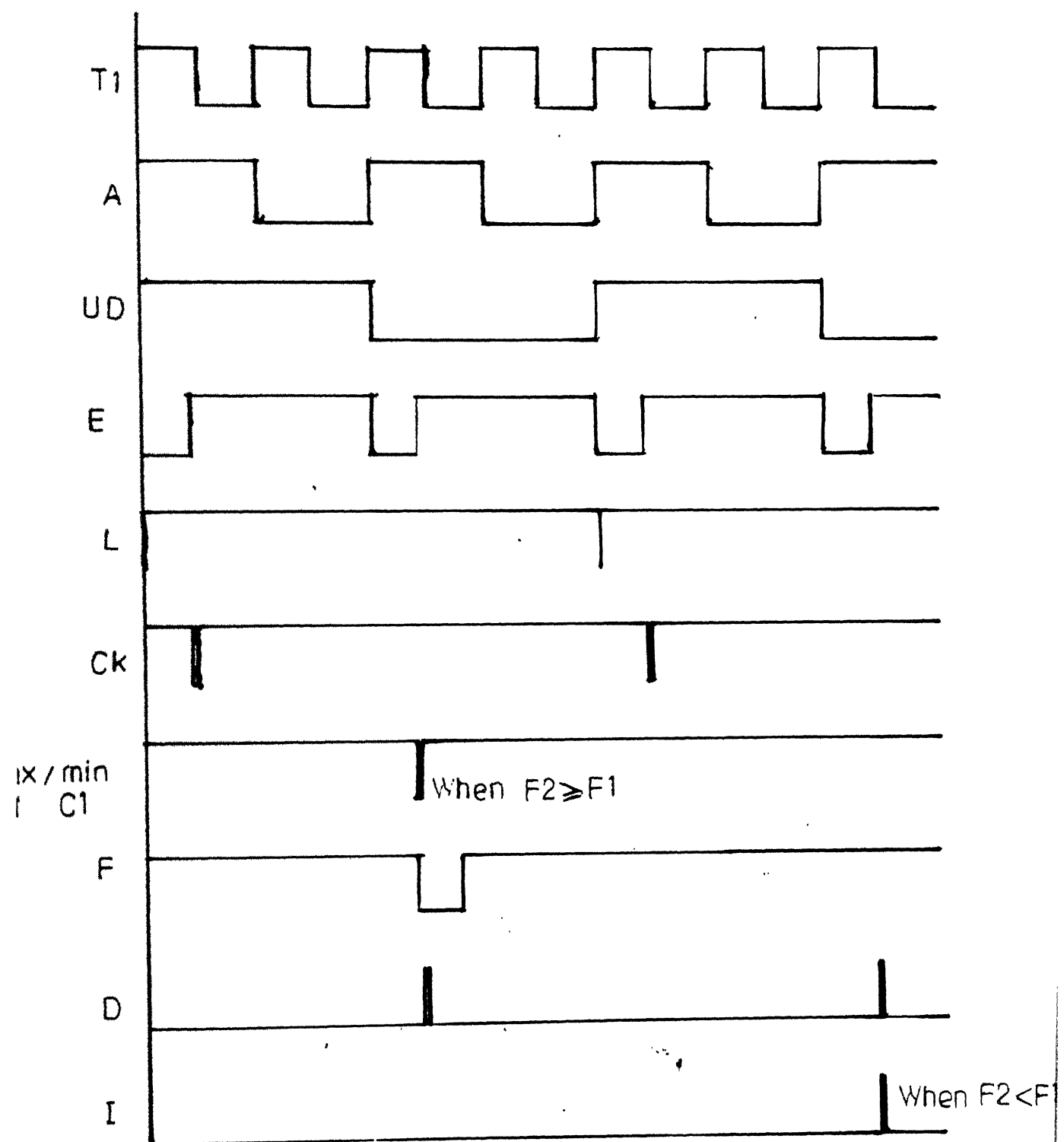


Fig. 4.4.2 Waveforms of maximum power tracker circuit

frequency of the VCO. If the output frequency of the VCO is either increased or remains the same then counter will produce a pulse at its ripple clock output which is used to block the pulse to, JK flipflop  $J_3$  and the cycle will be repeated. On the other hand if the output frequency of VCO is decreased no ripple clock pulse will produce. Then a pulse will be realised to JK flipflop  $J_3$  which will reverse the mode of counting of counter  $C_2$  and thereby direction of change in the modulation, and the cycle will be repeated.

#### 4.5 PROTECTION CIRCUIT

The power switches used in the inverter circuit must be protected against switching transient otherwise device may damage due to secondary breakdown [16]. Usually the polarised snubber circuits are used for this purpose. The protection circuits limits the rate of rise of current and the voltage within the prescribed limit at turn on and turn off of the switch. The snubber circuits are designed so that the power switch always operates within the safe operating area [SOA] prescribed by manufacturers and thus keeps the device heat dissipation low. The authors of references [17 and 18] have reported methods of calculation of the

snubbers circuit components in order to reduce losses in the device as well as the total switching loss. The inverter circuit with all protection circuits is shown in Fig. 4.5.1.

#### 4.5.1 Turn on Snubber Circuit:

The turn on snubber circuit is connected only with main transistor due to its high frequency of operation. The circuit consists a small inductance and a diode-resistance network as shown in Fig. 4.5.1. The inductance induces voltages equal to and of opposite polarity of the input voltage when the main transistor current begins to rise, thereby collapsing the collector emitter voltage to its saturation level. By assuming that the collector current rises linearly during time, the value of inductance can be calculated as follows:

$$V_{in} = \frac{L \cdot I}{T_r}$$

$$\text{or } L = \frac{V_{in} \cdot T_r}{I}$$

The network inductance is charged exponentially during the transistor turn off time by the voltage drop across the network resistance. The network resistance is selected to provide the shortest changing time interval consistent with

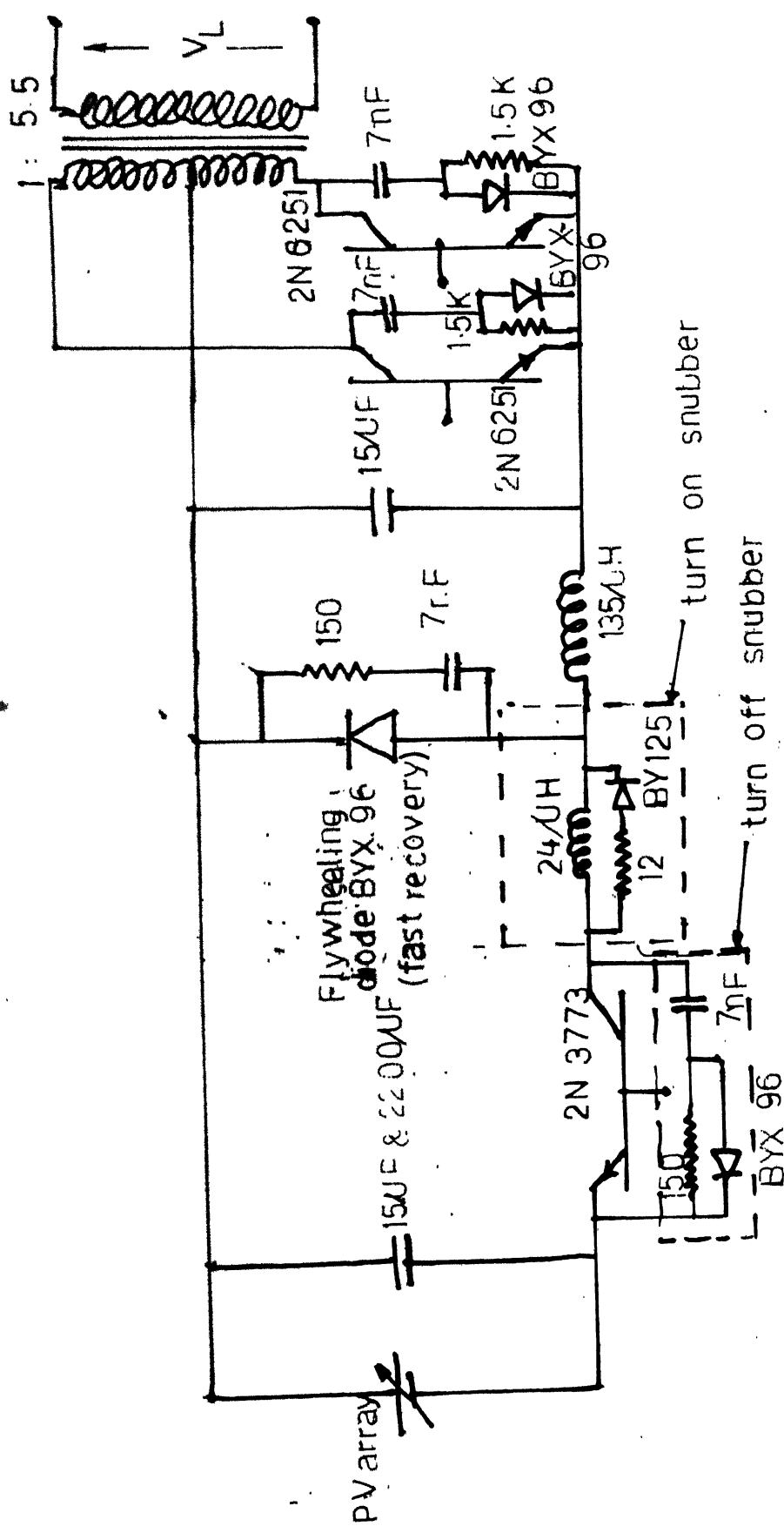


Fig. 4.5.1 Inverter circuit with snubbers

extra burden placed on the transistor by the charging voltage, which appears in series with it at turn off. An inductance of 24  $\mu$ H and a resistance of 12 Ohms <sup>are</sup> ~~was~~ selected for the inverter ratings ~~given in Appendix B.~~ of 2 Amp & 80 Volts

#### 4.5.2 Turn off Snubber Circuit:

A normal diode-resistance-capacitor network is used as a snubber during turn off. At turn off, the capacitor charges at a very fast rate through a diode and thus limits the rate of rise <sup>of</sup> the voltage. At turn on it discharges through a resistance to limit the discharge current. By assuming that during turn-off time <sup>T<sub>f</sub></sup> the collector voltage rises linearly from saturation voltage to input supply voltage. The value of capacitor C can be calculated as

$$V = \frac{1}{C} \int idt = \frac{1}{C} \int_0^{T_f} \frac{I}{T_f} t dt = \frac{1}{C} \frac{I}{T_f} \left[ \frac{t^2}{2} \right]_0^{T_f} = \frac{1}{C} \frac{I T_f^2}{2}$$

or

$$C = \frac{I T_f}{2V}$$

where  $V = V_{in} + \text{voltage drop across the network resistance.}$

The network resistance is selected to provide the shortest charging time interval consistent with the extra burden placed on the transistor by the discharge current.

at turn on. A capacitor of  $7 \text{ mF}$  and resistance of  $250 \text{ ohms}$  are selected for main transistor's snubber. However since  $T_1$  and  $T_2$  operate at a low frequency there is a large time interval available for changing of capacitor therefore larger resistance can be used to limit the discharge current. A network of  $7 \text{ mF}$  capacitors and  $1.5\text{K}$  resistance with a fast recovery diode are used for transistors  $T_1$  and  $T_2$ .

#### 4.6 EXPERIMENTAL SET UP

The complete control circuit was fabricated on a single PCB as shown in Fig. 4.6.1 and was fitted with power circuit of inverter in a proper metal assembly. Since induction motor and centrifugal pump were not available in the required power rating, a pedestal fan of  $60\text{W}$  was used. Two DPDT switches and two potentiometer were fitted at the front panel of the inverter assembly. By the help of switches the modulation index and frequency of inverter can be varied either in close loop or in open loop by manual adjustment. The following alternative operations are possible.

##### a) Modulation index and inverter frequency in open loop:

The level of the input voltage and power to the motor as well as inverter frequency can be adjusted to any desired value by setting the positions of potentiometer, which are fitted on the front panel of inverter.

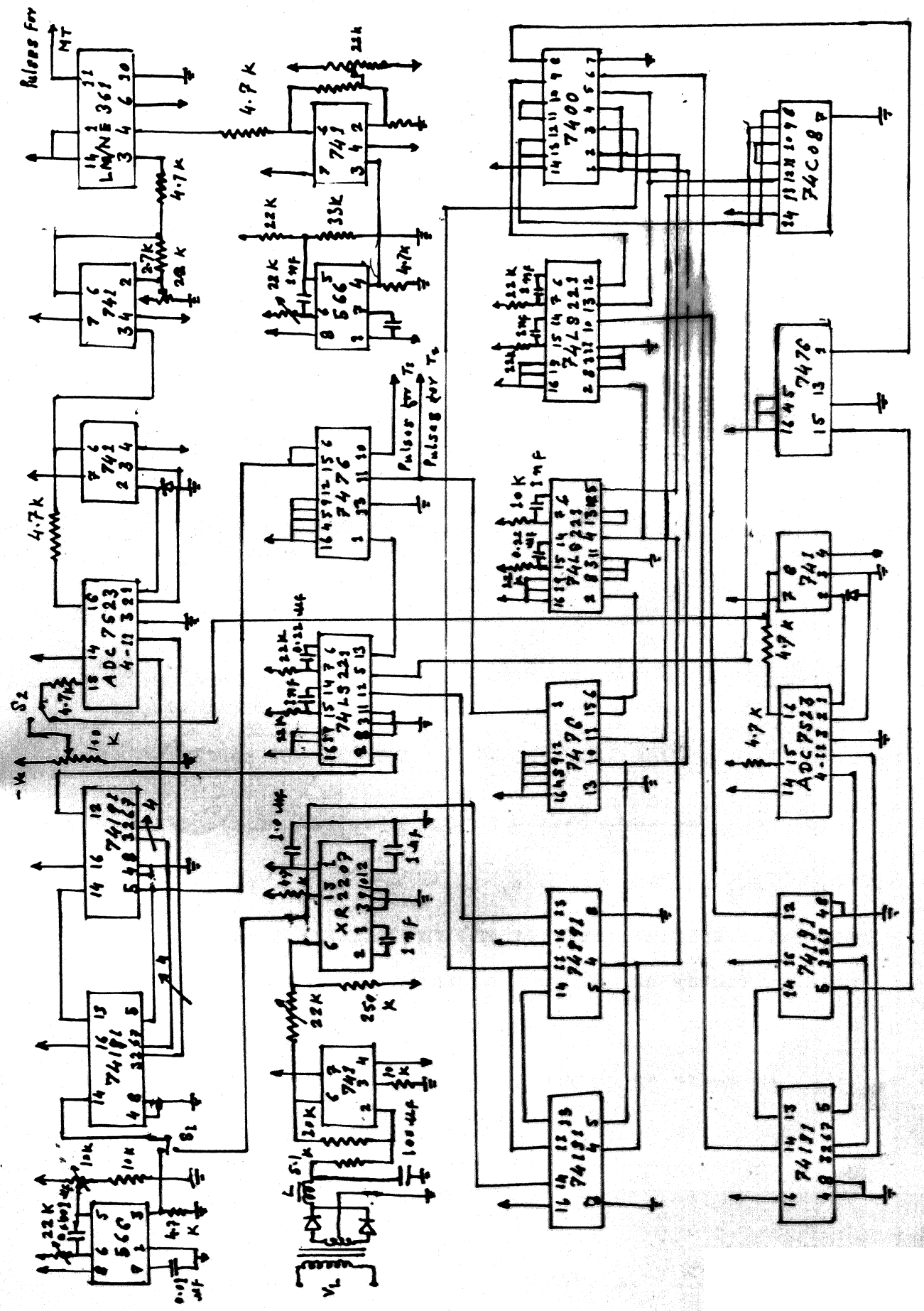


Fig. 4.6.1 Detailed control circuit

b) Modulation index in open loop and inverter frequency in close loop:

In this case the level of input voltage and power to the motor can be controlled with the help of a potentiometer, while inverter frequency is decided by the motor terminal voltage so that ratio between them is maintained at 4:4.

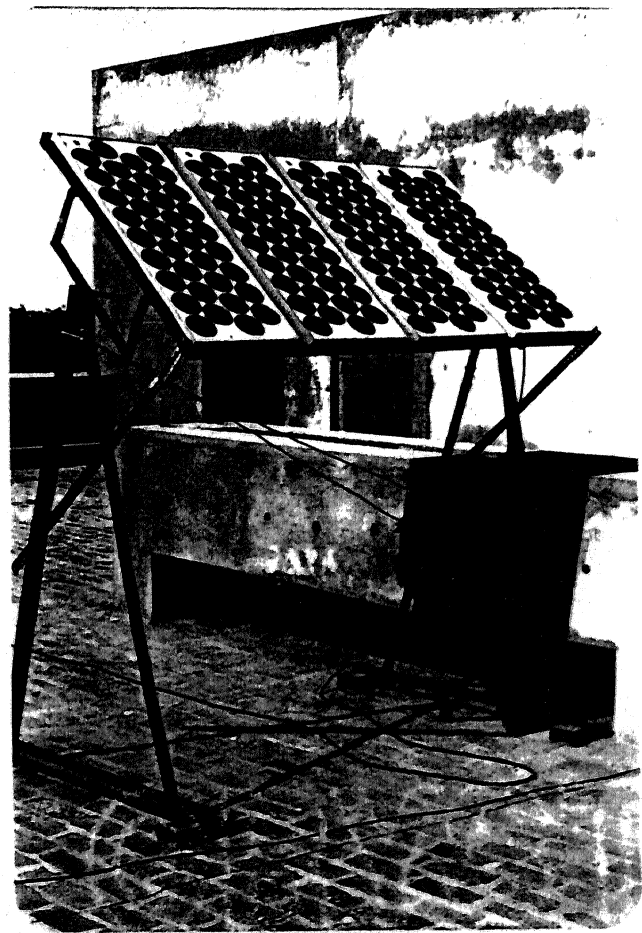
c) Modulation index in close loop and inverter frequency in open loop:

In this case input voltage and power to motor are maintained at the maximum possible value by maximum power buck circuit. The inverter frequency can be controlled by adjusting the setting of the potentiometer.

d) Modulation index and inverter frequency in close loop:

In this case the level of input voltage and power to the motor is maintained at the maximum possible value and inverter frequency is maintained by VCO to keep V/f ratio constant at 4.4.

The complete experimental set up is shown in Fig. 4.6.2.



Pl. area, in 'B'

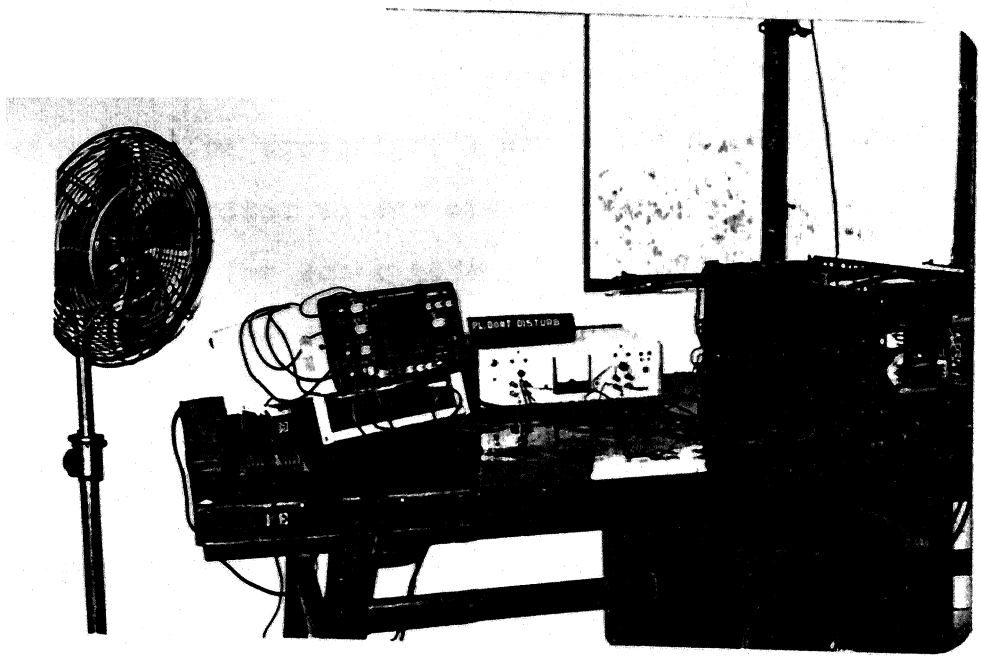


Fig. 10.2.1. Experimental setup

## CHAPTER 5

### PERFORMANCE OF THE DRIVE

#### 5.1 ANALYSIS OF SINGLE PHASE PERMANENT CAPACITOR MOTOR

The analysis of permanent capacitor induction motor is some what complicated than other single phase induction motors due to interaction of two fields and dissimilarity of the constants for two windings. Therefore no simple equivalent circuit can be drawn. The author in reference [19] has reported a method for analysis of this type of motor by using cross field theory. The two windings on stator are assumed to be in space quadrature. The winding having capacitor in series is designated as start winding. The subscript S and M are used for start and main winding respectively. The subscripts 1 and 2 are used for stator and rotor. All rotor values are expressed in terms of main stator winding. The subscripts y and x are used for rotor currents referred to stator main and start winding respectively.

The following notation are used:

stator main winding impedance  $= \frac{Z}{2IM}$

stator main winding current  $= IM$

stator main winding counter emf = EM

stator main winding magnetic impedance = ZM

stator start winding impedance = Z1S

stator start winding current = IS

stator start winding counter emf = ES

stator start winding magnetic impedance = ZS

impedance of capacitor = ZC

rotor impedance = Z2

rotor current refer to stator main winding = IY

rotor current refer to stator start winding = IX

rotor reactance = X2

start to main winding turn ratio = a

speed of rotor per unit synchronous speed = S

The following fundamental equations can be written.

For start main winding

$$V = Z_M (I_M - I_Y) + I_M Z_{1M} \quad (1)$$

counter emf impedance drop

For stator start winding

$$V = Z_S (I_S - I_X) + I_S (Z_{1S} + Z_C) \quad (2)$$

counter emf impedance drop

For rotor refer to main winding

$$\zeta_M (I_M - I_Y) + S[j \frac{Z_S}{a} (I_S - I_X) + a I_X x_2] - I_Y Z_2 = 0 \quad (3)$$

transformer voltage   speed  $\frac{V_U/f_{60}}{\text{emf}}$       impedance drop

For rotor refer to start winding

$$\frac{\zeta_S}{a} (I_S - I_X) + S[-j Z_M (I_M - I_Y) - I_Y x_2] - a I_X z_2 = 0 \quad (4)$$

transformer   speed voltage      impedance drop  
voltage

These four equations can be solved for  $I_M$ ,  $I_S$ ,  $I_Y$  and  $I_X$  than the performance of the motor can be calculated as follows.

Counter emf in main winding  $E_M = V - I_M Z_M$

Counter emf in start winding  $E_S = V - I_S (Z_S + Z_C)$

The rotor input or power transferred across the air gap is:

$$\rightarrow E_M I_Y \cos (E_M, I_Y) + E_S I_X \cos (E_S, I_X)$$

Power converted in to mechanical power = power transferred across the air gap -  
rotor copper loss

$$\rightarrow P_M = E_M I_Y \cos (E_M, I_Y) +$$
$$\rightarrow E_S I_X \cos (E_S, I_X) -$$
$$(I_Y^2 + a^2 I_X^2) R_2$$

Net output =  $P_M$  - friction and windage loss

The torque in synchronous walls can be given as

$$a E_M I_x \sin(E_M, I_x) + \frac{E_S}{a} I_y \sin(E_S, I_y)$$

and the stator input is

$$\rightarrow V_{IM} \cos(V_{IM}) + V_{IS} \cos(V_{IS})$$

total supply current

$$I = I_M + I_S$$

hence power factor =  $\cos(V, I)$

Two motors were analysed by using this method. The characteristics are shown in Fig. 5.1.1 to 5.1.2 for Motor I and Motor II respectively. The parameter of the motors were obtained from the no load and block rotor tests and are given in Appendix G. In the characteristics of motor I, it can be noted that the variation of the input current and power with speed is unusual. This may be due to small size of machine.

## 5.2 PERFORMANCE OF INVERTER

The inverter was tested on different types of loads namely resistive,  $\pi L$  and single phase permanent capacitor motor. The oscillograms of the output and input currents and voltages are shown in Fig. 5.2. This figure also shows

Characteristics of 1 ph. permanent capacitor induction motor

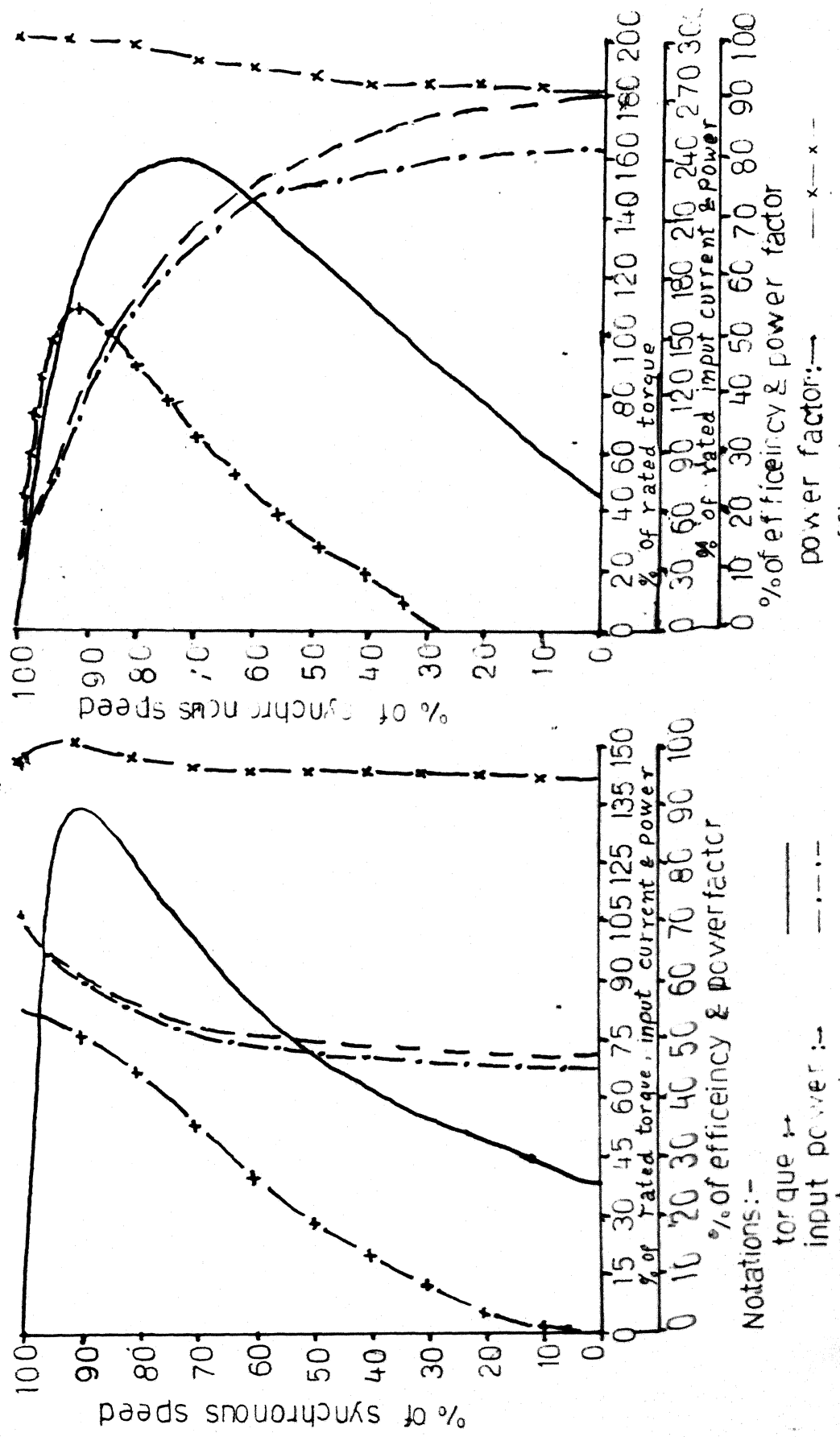
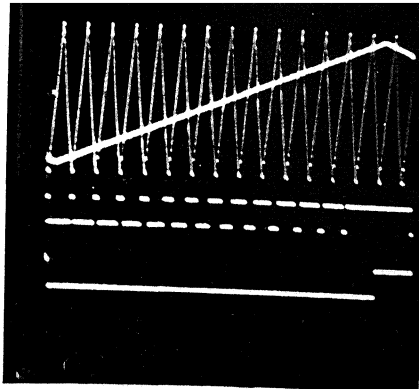


Fig. 5.1.1 Motor I

Fig. 5.1.2 Motor II



a. Firing circuit waveforms  
From top:-

- (i) Carrier wave (2V/div)
- (ii) Modulating wave (2V/div)
- (iii) PWM pattern (5 V/div)
- (iv) Up-down signal to counter (5 V/div)

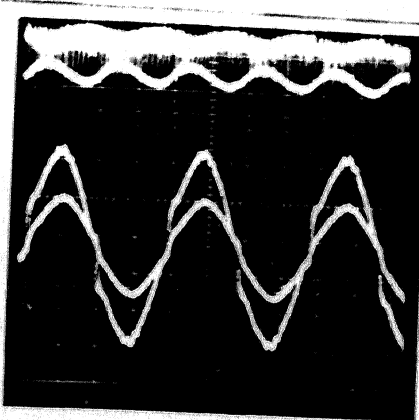
time scale: 0.2 msec/div.

b. Waveforms of inverter with resistive load (200 ohms).

From top:-

- (i) Input current (0.166 A/div)
- (ii) Input voltage (5 V/div)
- (iii) Output voltage (50 V/div)
- (iv) Output current (0.416 A/div)

time scale : 5 msec/div.  
reference level for DC: bottom line of graph.

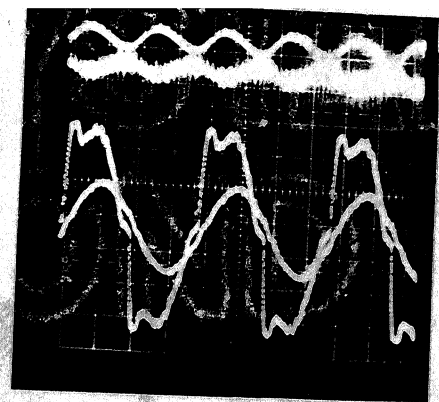


c. Waveforms of inverter with R-L load (200 ohms, 415 mH)

From top:-

- (i) Input voltage (5 V/div)
- (ii) Input current (0.166 A/div)
- (iii) Output voltage (50V/div)
- (iv) Output current (0.416A/div)

time scale: 5 msec/div.  
reference level for DC: bottom line of graph.



d. Waveforms of inverter with single phase capacitor run Induction motor.

From top:-

- (i) Input current (0.166 A/div)
- (ii) Input voltage (10 V/div)
- (iii) Output voltage (100 V/div)
- (iv) Output current (0.416 A/div)

time scale: 5 msec/div.  
reference level for DC: bottom line of graph.

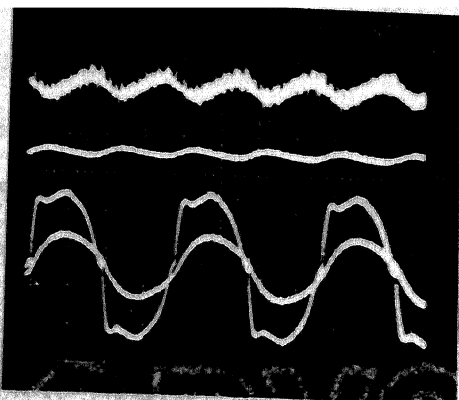


Fig. 5.2.1 Oscillations of inverter performance

an oscillogram of the half cycle of the PWM pattern. From the oscillograms, it can be seen that the output current wave shape is independent of the type of load and is very close to sinusoidal. The output voltage waveform depends upon the type of load. In the case of motor load, it is close to sinusoidal. However at the lower modulation index and frequency, considerable distortion in the output voltage and current wave forms was found. This may be due to <sup>use of</sup> triangular reference waveform instead of sinusoidal. The ripples in the input voltage and currents are considerably low.

### 5.3 PERFORMANCE OF DRIVE

In the present drive, two speed control schemes, namely stator voltage control at fixed frequency and constant V/F ratio control are implemented. A maximum power tracker circuit is used to <sup>maximize</sup> minimize the input power to the motor by controlling the modulation index. In order to check the performance of the maximum power tracker circuit, option for open loop control of the modulation index is also provided. Since short circuit current of the solar cell is proportional to the intensity of the light, the speed of the fan, power input to motor and power output of PV array are measured at different values of short circuit current by using both schemes of the speed control.

with and without maximum power tracker circuit, and are given in table I. When maximum power tracker is not used, the input power to the motor is adjusted to a maximum value with the help of potentiometer.

From the results of Table I, it can be seen that maximum power tracker is capable of maintaining the input power to the motor within 2% of the 'maximum value'. However it did not make full use of maximum available PV power, especially at low power levels. At low insolation levels stator voltage control with fixed frequency gives higher speed of the fan than the constant V/F ratio control. While at higher insolation levels constant V/F ratio gives better results. This may be due to the fact that the current required by motor with constant V/F ratio may be more than that with fixed frequency stator voltage control at low speeds, which may force the array to operate at lower voltage and power levels. Since the input current to the motor attains a maximum value at about 2/3 of synchronous speed with stator voltage control, the required current may be more than that with constant V/F ratio at higher insolation levels. This may be the reason of lower speeds at higher insolation level with stator voltage control. Since the power output of the

Table 1: EXPERIMENTAL RESULTS

Port circuit ip.	Max. available power Watts	Stator voltage control			Manual			with maximum power tracker			Constant V/F ratio constant		
		Speed Power out- put of PV array	In- put of Power from PV array	In- put of fan power from PV array	Speed of fan rpm	In- put of power from PV array	In- put of fan power from PV array	Speed of fan rpm	In- put of power from PV array	Speed of fan rpm	In- put of power from PV array	Speed of fan rpm	In- put of power from PV array
.78	32.0	22.0	10.0	61	22.0	10.0	62	14.0	4.0	—	13.0	4.0	—
.02	49.0	36.0	19.0	375	37.0	19.0	360	35.0	11.0	160	36.0	11.0	180
.12	52.0	52.0	21.0	330	51.0	20.0	340	30.0	12.0	120	42.0	15.0	240
.14	50.0	41.0	20.0	270	41.0	20.0	265	27.0	8.0	30	30.0	12.0	95
.18	54.0	51.0	22.0	540	50.6	22.0	525	50.0	22.0	836	50.0	21.0	782
.30	60.0	56.0	28.0	780	57.0	29.0	790	62.0	28.0	1000	63.0	32.0	1007
.33	60.0	55.0	2760	732	57.0	28.0	740	55.0	27.0	932	56.0	27.0	920
.41	62.0	60.0	31.0	840	61.0	32.0	880	65.0	32.0	1037	65.0	33.0	1045
.48	64.0	64.0	32.0	862	64.0	32.0	856	64.0	28.0	1070	64.0	24.0	1080
.51	66.0	65.0	34.0	990	66.0	38.0	970	66.0	36.0	1090	65.0	36.0	1090

fan is proportional to the cube of its speed and short circuit current of a <sup>solar</sup> roter cell is proportional the to the intensity of the light, a direct relation between power output of fan and intensity of light can be obtained from Table I.

## CHAPTER 6

### CONCLUSIONS

A photovoltaic induction motor drive was built and tested in the laboratory with a fan load. A maximum power tracker was used to maximize the input power to the motor. The suitable speed control schemes were used to ensure good efficiency of the motor. The performance of the maximum power tracker was found to be satisfactory. The results reveal that at low insolation level, stator voltage control gains higher motor speed, while constant V/F ratio control gives better results at higher insolation levels. The analysis of the system for efficiency and operation of drive with pump could not be undertaken due to limitation of time and unavailability of pump in desired ratings. However the test on the fan in lab. indicates that drive scheme is suitable for small photovoltaic pump systems.

The present scheme has certain disadvantages which require further investigations. In this scheme stepped <sup>reference</sup> triangular modulation waveform was used to generate PWM pattern which results not only in distortion of the output voltage and current waveforms of inverter at low values of modulation index and frequency but also affects the performance of VCO and maximum power tracker circuit, because the relation between

peak and rms values of motor terminal voltage does not remain the same for all values of modulation index. This problem can easily be eliminated by using sinusoidal reference wave instead of stepped triangular. Further more at low ~~radiation~~ <sup>insolation</sup> levels, none of the speed control scheme ensures full utilization of the maximum <sup>available</sup> variable photovoltaic power. A speed control scheme may be investigated which should control the speed of drive in such a way that the current required by the motor should be slightly, less than the photovoltaic current corresponding to the maximum power point at all insolation levels and temperatures. Further more to ensure maximum mechanical output (water), speed of the drive can be maximized instead of input voltage to the motor. It will be interesting to perform efficiency analysis of induction motor pump systems and its comparison with other available PV pump drive systems.

## APPENDIX I

### RATINGS AND PARAMETERS OF MOTORS

#### Motor I

hating 220/240 volts, 40 Watt padstal fan

#### Parameters

stator main winding resistance  $R_{IM}$  = 189.87 ohm

stator main winding reactance  $X_{IM}$  = 237.056 ohm

stator main winding magnetizing reactance  $X_{MM}$  = 1025.31 Ohm

Stator start winding resistance  $R_{IS}$  = 229.665 ohm

stator start winding reactance  $X_{IS}$  = 266.879 ohm

stator start winding magnetizing reactance  $X_{MS}$  = 2031.39 ohm

reactance of capacitor  $X_C$  = 1327.258 ohm

equivalent series resistance of capacitor  $R_C$  = 4.896 ohm

rotor resistance refer to stator  $R_2$  = 130.122 ohm

rotor reactance refer to stator  $X_2$  = 237.056 ohm

equivalent core resistance of main winding  $R_{MM}$  = 7523.9061 ohm

equivalent core resistance of start  $R_{MS}$  = 14905.18 ohm

startion main winding turn ratio  $a$  = 1.4075 ohm

friction and windage  $\cancel{or}$  loss = 1.50 watts.

## Motor II

0.25 HP, permanent capacitor induction motor and centrifugal pump in mono block.

### ratings

220/240V, 50 Hz, 1.8A, 2700 rpm, 0.25 HP, 4.5/14 mt,  
64/28 lpm

### Parameters

stator main winding resistance  $R_{IM}$  = 19.04 ohm

stator main winding reactance  $X_{IM}$  = 11.028 ohm

stator main winding magnetizing reactance  $X_{MM}$  = 299.027 ohm

stator main core loss equivalent resistance  $R_{MM}$  = 1174.32 ohm

stator start winding resistance  $R_{IS}$  = 18.904 ohm

stator start winding reactance  $X_{IS}$  = 9.9116 ohm

stator start winding magnetizing reactance  $X_{MS}$  = 344.50 ohm

stator start winding core loss equivalent resistance  $R_{MS}$  = 1025.6

rotor resistance refer to stator side  $R_2$  = 19.54 ohm

rotor reactance refer to stator side  $X_2$  = 11.028 ohm

reactance of capacitor  $X_C$  = 344.50 ohm

equivalent series resistance of capacitor  $R_C$  = 8.277 ohm

friction and windage loss  $FWL$  = 29.0 watts.

where,

$$ZIM = RIM + j XIM$$

$$ZM = RMM//j XMM$$

$$ZIS = RIS + j XIS$$

$$ZS = RMS//j X M$$

$$ZC = RC + j XC$$

$$Z_2 = R_2 + j X_2$$

## REFERENCES

- [1] Buresch, Mathew, 'Photovoltaic Energy Systems', McGraw-Hill Book Company, 1983.
- [2] Green Martin A., 'Solar Cells', Prentice Hall Inc. Englewood Cliffs, N.J. 1982.
- [3] S.M. Sze, 'Physics of semiconductor devices', Wiley Eastern Ltd. 1985.
- [4] Chenming HV, Richard M. White, 'Solar Cells from Basic to Advance Systems', McGraw-Hill Book Company, 1983.
- [5] Bimal K. Bose, Paul M. Szezesny and Robert L. Steigerwald, 'Microcomputer control of a residential photovoltaic power conditioning system', IEEE Trans on Ind. App. vol. IA-21, No. 5, pp. 1182-91, Sept/Oct. 1985.
- [6] Urs Boegli and Hemo Ulmi, 'Realization of a new inverter circuit for direct photovoltaic energy feedback into the public grid', IEEE Trans. on Ind. App., vol. IA-22, No. 2, pp. 255-58, March/April, 1986.
- [7] 'Small scale solar-powered irrigation pumping systems phase I project report', UNDP Project GLO/78/004, Executed by the World Bank, July, 1981.
- [8] G.K. Dubey and W.G. Dunford, 'Solar Pump drives', A project report, University of British Columbia.
- [9] J. Appelbaum and J. Bany, 'Performance analysis of d.c. motor photovoltaic converter system-I separately excited motor', Solar Energy, vol. 22, No. 5, pp. 439-445, 1979.
- [10] J. Appelbaum, 'Performance analysis of dc motor photovoltaic converter system-II series and shunt excited motors', solar energy, vol. 27, No. 5, pp. 421-431, 1982.
- [11] A. Braunstein and A. Kornfield, 'Analysis of Solar Powered electric water pumps', Solar energy vol. 27, No. 3, pp. 235-240, 1981.

- [12] Joseph R. Pottebaum, 'Optimal characteristics of a variable frequency centrifugal pump motor drive', IEEE Trans. on Ind. App., vol. IA-20, No. 1, pp. 23-31, Jan/Feb. 1984.
- [13] Cyril G. Veinott, 'Fractional and subfractional horse power electric motors', McGraw-Hill Book Company, 1970.
- [14] P. Savary, M. Nakaoka and T. Maruhashi, 'Novel type of high frequency link inverter for photovoltaic residential applications', IEE Proc. vol. 133, Pt. B, No. 4, pp. 229-284, July, 1986.
- [15] Mitsuaki Homby, Shijeta Veda, Akiteru Veda and Yasud Matsui, 'A New current source GTO inverter with sinusoidal output voltage and current.
- [16] Wood Peter, 'Switching Power Converter', Van Nostrand Reinhold Company, 1981.
- [17] E.T. Calkin and B.H. Hamilton, 'Circuit techniques for improving the switching loci of transistor switches in switching regulators', IEEE Trans on Ind Appl., vol. IA-12, No. 4, pp. 364-69, July/Aug. 1976.
- [18] E.T. Calkin and B.H. Hamilton, 'A conceptually new approach for regulated DC to DC converters employing transistor switches and pulse width control', IEEE Trans. on Ind. Appl., vol. IA-12, No. 4, pp. 369-77, July/Aug. 1976.
- [19] A.F. Puchstein, T.C. Lloyd and A.G. Conard, 'Alternating - current machines', Third edition, John Wiley and Sons, Inc., New York, 1960.

A 88326

## Thesis

621.31244

J184

**Date Slip**

A 98326

This book is to be returned on the  
date last stamped.

EE-1987-M-JAF-PHO